

Ultraheavy resonances at the LHC: beyond the QCD background

Bogdan A. Dobrescu, Robert M. Harris and Joshua Isaacson

Fermi National Accelerator Laboratory, Batavia, Illinois 60510, USA

(Dated: October 22, 2018)

We study the theory and some experimental hints of ultraheavy resonances at the LHC. The production of an ultraheavy narrow particle may have a larger rate than the QCD background even when the final state includes only hadronic jets. We consider two classes of models that lead to 4-jet signals. In the first class a diquark scalar decays into two vectorlike quarks. In the second one a coloron decays into two color-octet scalars or into a pair of vectorlike quarks. We show that a diquark as heavy as 11.5 TeV, or a coloron as heavy as 8.5 TeV may be discovered at the LHC. We point out that a CMS 4-jet event may be due to an 8 TeV resonance decaying into two secondary particles, each with a mass of 1.8 TeV. We find that the QCD background with a 4-jet mass and dijet masses that equal or exceed those of the CMS event is approximately 5×10^{-5} events in 78 fb^{-1} of data, while the diquark signal could have easily produced that event. The diquark also decays directly into two jets, which may be the origin of some of the three other events of mass near 8 TeV observed by ATLAS and CMS.

Contents

I. Introduction	2
II. Diquark scalar plus vectorlike quark	5
A. Scalar interacting with two up quarks	5
B. S_{uu} diquark production and a dijet resonance at the LHC	6
C. Up-type vectorlike quark and a 4-jet scalar resonance	8
D. QCD 4-jet background	11
III. Coloron plus scalar or vectorlike quark	14
A. Coloron production	14
B. Coloron signals with resonant pair of dijets	16
IV. Events with a mass of 8 TeV	20
A. Dijet and 4-jet LHC searches and events	20
B. QCD background to resonant production of a pair of dijets	23
C. Signals of an 8 TeV particle	28
1. S_{uu} diquark with a mass of 8 TeV	28
2. Other models	33
V. Conclusions	35
References	37

I. INTRODUCTION

The ATLAS and CMS experiments at the LHC have been pushing the limits of the Standard Model (SM) to higher and higher energies over the last eight years. New particles that can be produced in the s channel have a large production cross section due to resonant enhancement, and yet may be narrow enough to be easily observed above a smooth background. For example, the lower limit from dijet resonance searches (for reviews, see [1–3]) on the mass of a Z' boson that couples to quarks the same way as the Z boson has increased

from 0.74 TeV before the start of the LHC [4] to 1.7 TeV at the end of the 8 TeV run of the LHC [5], and is now 2.7 TeV [6]. It is compelling to ask what is the highest-mass resonance that can be discovered or excluded by the end of the upcoming high-luminosity run of the LHC.

Particles of mass above a few TeV that couple to two quarks, usually called diquarks, are expected to be produced with the highest cross section while still having a narrow width. The reason is that the parton distribution functions (PDFs) of the up and down quarks are much larger than those of other proton constituents when the momentum carried by the parton is large. While it is difficult to construct a renormalizable theory that includes a spin-1 diquark (see *e.g.*, [7]), spin-0 diquarks can easily be included in renormalizable extensions of the SM. In particular, color-sextet diquarks [8–10] that couple to uu or ud have the largest production cross section.

Even though resonances produced from quark-antiquark initial states have smaller production rates, they are still particularly interesting as they probe the existence of gauge bosons beyond the SM. Among possible new gauge bosons, the coloron (a spin-1, color-octet particle) has the special feature that it is associated with a non-Abelian gauge group which may be asymptotically free. As a result, the coloron coupling to quarks may be relatively large in a completely specified renormalizable theory, especially if its interactions are flavor-independent [11]. By contrast, other gauge bosons, such as a Z' , cannot have a large coupling unless the UV completion at a scale near the gauge boson mass is some unidentified strongly coupled theory. The coloron is associated with an extension of the QCD gauge group: $SU(3)_1 \times SU(3)_2$, which is spontaneously broken down to its diagonal subgroup, $SU(3)_c$, responsible for the massless gluon. The simplest origin of the spontaneous symmetry breaking is a scalar field Σ that transform as $(3, \bar{3})$ under the extended gauge group. The theory with the most general renormalizable potential for Σ is referred to as the Renormalizable Coloron Model (ReCoM) [12–14].

In this article we study theories with either a diquark scalar or a coloron of mass above half the collider center-of-mass energy, which can nevertheless be sufficiently weakly coupled to have a narrow width. We show that such ultraheavy narrow resonances can be produced with a rate larger than that of the QCD background even when the final state consists only of jets. After estimating the ultimate reach of the LHC in searches for narrow dijet resonances of these types, we consider the decay of the ultraheavy particle in a pair of new TeV-scale

particles. Specifically, we introduce a vectorlike quark which interacts in pairs with the diquark or the coloron, and decays predominantly into two jets. Thus, the signature is an ultraheavy 4-jet resonance, with each of two pairs of jets forming a dijet resonance of mass equal to that of the vectorlike quark. A similar signature arises in the ReCoM from the coloron decay into scalars that are part of the symmetry breaking field Σ . Related processes in strongly coupled theories have been studied in [16, 17].

The CMS search for dijet resonances [6] has reported an unusual event, with four jets forming a resonance at 8.0 TeV. Those four jets are grouped in two wide jets with equal masses, of 1.8 TeV. We compute the probability that this event is due to QCD and find that it is approximately 5×10^{-5} . We show that this event is consistent with a diquark decaying into a pair of vectorlike quarks, each then decaying into two jets. The diquark also has a decay mode into two jets, which may lead to an excess of dijet events of mass near 8 TeV. The same CMS search reported a dijet event of mass at 7.9 TeV, while the latest ATLAS search for dijet resonances [18] reported two dijet events of mass in the 8.0–8.1 TeV range. Nevertheless, these three dijet events may be due to a modest upward fluctuation of the QCD background.

We will not be concerned with underlying principles that may motivate the presence of the new particles discussed here. We note though in passing that the color-sextet diquark scalars and vectorlike quarks are part of the 126 representation of the supersymmetric $SO(10)$ grand unification [19]. Theories that include a coloron and a vectorlike quark have been studied especially in conjunction with composite Higgs models. In fact, the term ‘coloron’ has been introduced [20] in the context of Higgs compositeness, and later it was shown that natural models of this type must also include a vectorlike quark [21].

In Section II we present the diquark model and compute the signal and background cross sections. The coloron model and its signatures are analyzed in Section III. The events of mass near 8 TeV are discussed in Section IV. Our conclusions are included in Section V.

II. DIQUARK SCALAR PLUS VECTORLIKE QUARK

Let us consider a complex scalar field S_{uu} which is a color-sextet of electric charge $4/3$. More precisely, S_{uu} transforms under the SM gauge group $SU(3)_c \times SU(2)_W \times U(1)_Y$ as $(6, 1, +4/3)$, so that the only allowed renormalizable couplings of S_{uu} to SM fermions are Yukawa interactions to right-handed up-type quarks.

A. Scalar interacting with two up quarks

The interaction of the scalar diquark to two up quarks is required to produce S_{uu} at the LHC with a large rate. We assume that a flavor symmetry is acting on right-handed up-type quarks such that S_{uu} couples only to the first generation:

$$\frac{y_{uu}}{2} K_{ij}^n S_{uu}^n \bar{u}_{Ri} u_{Rj}^c + \text{H.c.} \quad (2.1)$$

Here y_{uu} is a dimensionless coupling. Without loss of generality we take $y_{uu} > 0$, because any complex phase may be absorbed in a redefinition of the u_R or S_{uu} fields. The factor of $1/2$ is conventional for interactions that involve two fields of the same type. The upper script c denotes the charge conjugated field. The i and j indices on the quark fields label the triplet color states ($i, j = 1, 2, 3$), and the upper index n on the scalar field labels the sextet color states ($n = 1, \dots, 6$). The coefficients K_{ij}^n are products of $SU(3)_c$ generators, which can be written as [22][9]

$$\begin{aligned} K_{ij}^1 &= \delta_{i1}\delta_{j1} \quad , \quad K_{ij}^2 = \frac{1}{\sqrt{2}} (\delta_{i1}\delta_{j2} + \delta_{i2}\delta_{j1}) \quad , \quad K_{ij}^3 = \delta_{i2}\delta_{j2} \quad , \\ K_{ij}^4 &= \frac{1}{\sqrt{2}} (\delta_{i2}\delta_{j3} + \delta_{i3}\delta_{j2}) \quad , \quad K_{ij}^5 = \delta_{i3}\delta_{j3} \quad , \quad K_{ij}^6 = \frac{1}{\sqrt{2}} (\delta_{i1}\delta_{j3} + \delta_{i3}\delta_{j1}) \quad , \end{aligned} \quad (2.2)$$

where δ_{ij} is the Kronecker symbol.

An example of flavor symmetry that prevents the coupling of the diquark to charm and top quarks is a global $U(1)$ with both u_R and S_{uu} charged under it. The mass of the up quark then must arise from a higher-dimensional operator of the type $\phi_u H \bar{Q}_L u_R$, where Q_L is a SM quark doublet, H is the SM Higgs doublet, and ϕ_u is a scalar field which has a VEV and is charged under the global $U(1)$. That higher-dimensional operator provides an explanation for the smallness of the up quark mass. The flavor symmetry is convenient because it reduces the number of parameters as well as the number of diquark decay modes. More important, it eliminates potentially large flavor-changing neutral processes [23].

The diquark interaction in Eq. (2.1) leads to the $S_{uu} \rightarrow uu$ decay. To leading order (LO), the width for this process is

$$\Gamma(S_{uu} \rightarrow uu) = \frac{y_{uu}^2}{32\pi} M_S . \quad (2.3)$$

If there are no other particles coupled to the diquark, then its total width, Γ_S , is given by $\Gamma(S_{uu} \rightarrow uu)$. We are interested in a relatively narrow resonance, that produces a well defined peak in the invariant mass distribution. We will focus on a diquark with a total width of up to 7% of its mass. This allows the use of the narrow width approximation in the computation of rates (for a recent study of the departures from the narrow width approximation see [24]). Furthermore, this constraint on the width-to-mass ratio implies that the experimental resolution, about 4% in CMS [25] for dijet resonances in the ultraheavy regime, is larger than the half-width. Thus, for comparison with the data, only the resolution determines the mass range over which the predicted background should be integrated. The constraint $\Gamma_S/M_S < 7\%$ translates to $y_{uu} < 2.7$.

B. S_{uu} diquark production and a dijet resonance at the LHC

Next we analyze the production of the S_{uu} scalar at the LHC. The partonic cross section for S_{uu} production at LO is given by

$$\hat{\sigma}(uu \rightarrow S_{uu}) = \frac{\pi}{6} y_{uu}^2 \delta(\hat{s} - M_S^2) , \quad (2.4)$$

where $\sqrt{\hat{s}}$ is the center-of-mass energy of the partonic collision. The cross section for S_{uu} production in proton-proton collisions of energy \sqrt{s} is

$$\sigma(pp \rightarrow S_{uu}) = \frac{2}{s} \int_0^1 \frac{dx}{x} \int_0^{sx} d\hat{s} u(x, M_S^2) u(\hat{s}/(sx), M_S^2) \hat{\sigma}(uu \rightarrow S_{uu}) , \quad (2.5)$$

where $u(x, Q^2)$ is the PDF of the up quark carrying momentum fraction x . The LO production cross section is

$$\sigma(pp \rightarrow S_{uu}) = \frac{\pi}{6s} y_{uu}^2 \int_{M_S^2/s}^1 \frac{dx}{x} u(x, M_S^2) u(M_S^2/(sx), M_S^2) . \quad (2.6)$$

Note that the production of S_{uu}^\dagger , the antiparticle of S_{uu} , leads to similar final states, but its cross section is much smaller because at partonic level it is due to $\bar{u}\bar{u} \rightarrow S_{uu}^\dagger$, and the PDF of \bar{u} is much smaller than the one for the up quark.

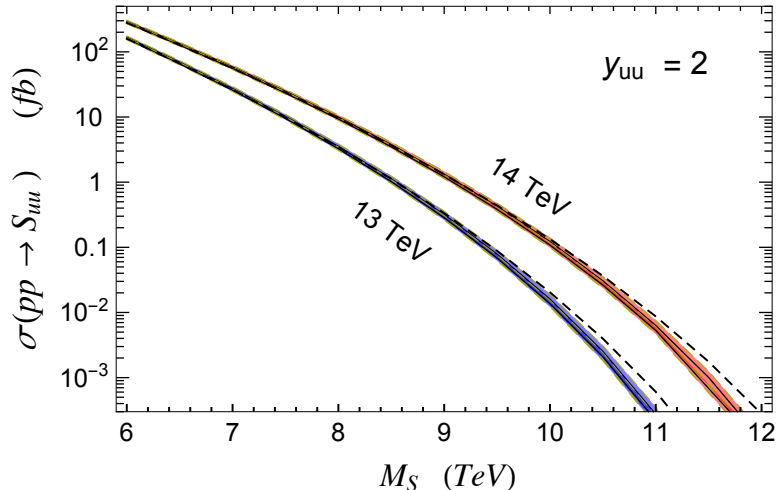


FIG. 1: Cross section for inclusive S_{uu} diquark production at $\sqrt{s} = 13$ TeV (blue band) and 14 TeV (red band), computed at NLO as a function of the S_{uu} mass. The diquark coupling is fixed here at $y_{uu} = 2$, which corresponds to a width $\Gamma(S_{uu} \rightarrow uu)/M_S = 4\%$ (the cross section scales as y_{uu}^2). The bands cover the central values obtained with the PDF sets CT14 [26] and MMHT2014 [27] at NLO, as well as their 1σ uncertainties. The black dashed lines represent the central values obtained with the NNPDF3.1 set [28] at NLO.

The next-to-leading-order (NLO) QCD corrections to diquark production have been computed in [9], and yield an increase of about 16% over the LO result. Using the full analytic expression for the NLO cross section, we find the predicted S_{uu} production cross section at the LHC shown in Figure 1: the blue band is for $\sqrt{s} = 13$ TeV, while the red band is for $\sqrt{s} = 14$ TeV. We used the current PDF sets at NLO from both CT14 [26] and MMHT2014 [27]; each band covers the values obtained with both sets as well as their uncertainties at the 68% CL. For comparison, the central values obtained with the PDF set NNPDF3.1 [28] at NLO are shown as dashed black lines. The cross sections obtained with NNPDF3.1 become notably higher than the ones obtained with CT14 or MMHT2014 only for $M_S/\sqrt{s} \gtrsim 0.8$. The PDF values and uncertainties were obtained through the use of the LHAPDF6 code [29].

The coupling of S_{uu} to up quarks is fixed in Figure 1 at $y_{uu} = 2$, but the results shown there can be easily scaled by y_{uu}^2 to obtain the cross section for any other value of the coupling. Note that $y_{uu} = 2$ corresponds to $\Gamma(S_{uu} \rightarrow uu)/M_S = 4\%$, while the total width for S_{uu} is 7% of its mass if it also couples to a vectorlike quark as discussed in Section II C.

Let us estimate the ultimate reach of the LHC in searches for the $pp \rightarrow S_{uu} \rightarrow jj$ process,

where each j is a jet obtained from the hadronization of an up quark. If there are no other new particles that S_{uu} can decay into (such as the vectorlike quark of Section II C), then $S_{uu} \rightarrow jj$ has a branching fraction very close to 100%. The QCD background to a dijet resonance search at the 14 TeV LHC has been estimated in [30] for jets of $|\eta_j| < 2.5$ and a pseudorapidity separation of the two jets $|\Delta\eta_{jj}| < 1.3$. Taking a mass window of 8% around the resonance mass, the background has a cross section of about 4.8 fb at a mass of 6 TeV, and decreases to about 0.13 fb at a mass of 8 TeV. The acceptance for a scalar resonance to pass the kinematic cuts mentioned above is around 1/2. The signal cross section times the acceptance is $30y_{uu}^2$ fb for $M_S = 6$ TeV and $1.1y_{uu}^2$ fb for $M_S = 8$ TeV. Thus, the signal-to-background ratio is already large (approximately $6.2y_{uu}^2$) at $M_S = 6$ TeV, and it grows with the resonance mass.

For $y_{uu} \gtrsim 1$ and $M_S \gtrsim 8$ TeV, the background is so much smaller than the signal that the $|\Delta\eta_{jj}|$ cut may be removed. In that case the acceptance increases to about 0.9. It is remarkable that for an S_{uu} mass as large as 11.3 TeV, the production cross section at the 14 TeV LHC obtained with the CT14 set is approximately 2×10^{-3} fb when $y_{uu} = 2$, which is large enough for about five dijet events to be observed with the anticipated 3000 fb^{-1} of data. For the largest value of the coupling consistent with $\Gamma_S/M_S < 7\%$, namely $y_{uu} = 2.7$, an S_{uu} diquark as heavy as 11.5 TeV may be discovered at the LHC.

C. Up-type vectorlike quark and a 4-jet scalar resonance

Besides the S_{uu} scalar, we now introduce another particle beyond the SM: a vectorlike quark χ , which has the same SM gauge charges as u_R , namely $(3, 1, +2/3)$. Given that the right- and left-handed components of χ have the same gauge charges, there are two renormalizable interactions of χ with the diquark scalar, which are analogous to Eq. (2.1):

$$\frac{1}{2} K_{ij}^n S_{uu}^n (y_{\chi_R} \bar{\chi}_{Ri} \chi_{Rj}^c + y_{\chi_L} e^{i\beta_\chi} \bar{\chi}_{Li} \chi_{Lj}^c) + \text{H.c.} \quad (2.7)$$

Since any complex phase of the coupling parameter y_{χ_R} may be absorbed in the χ_R field, we take $y_{\chi_R} \geq 0$. The phase of the χ_L field is then fixed by the mass term $m_\chi \bar{\chi}_R \chi_L$, so the complex phase of the second term in Eq. (2.7) cannot be removed. The coefficient of that term, $y_{\chi_L} e^{i\beta_\chi}$, is the most general one with the dimensional parameters satisfying $y_{\chi_L} \geq 0$ and $0 \leq \beta_\chi < 2\pi$.

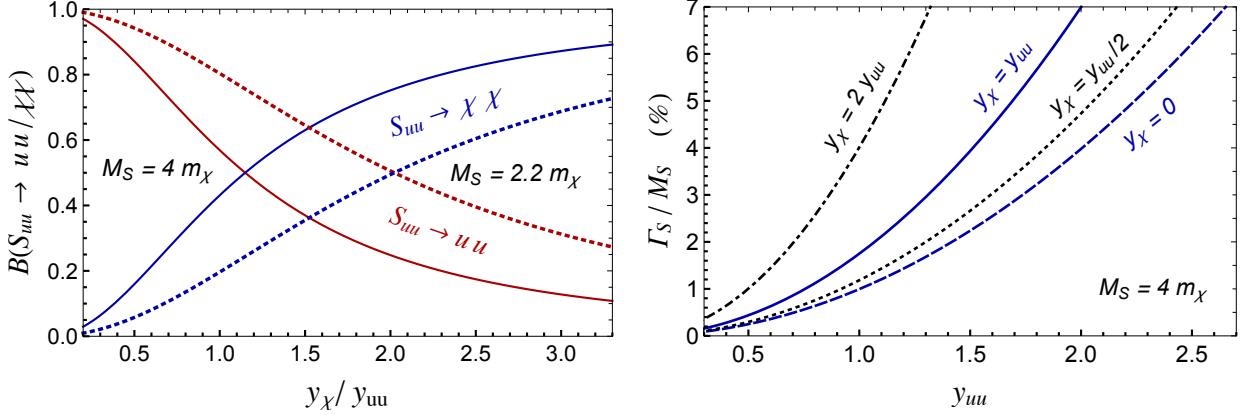


FIG. 2: *Left panel:* Branching fractions of the S_{uu} diquark as a function of the combination of couplings y_χ/y_{uu} , where $y_\chi \equiv \sqrt{y_{\chi R}^2 + y_{\chi L}^2}$, for a vectorlike quark mass $m_\chi = M_S/4$ (solid lines) or $M_S/2.2$ (dotted lines). *Right panel:* Width-to-mass ratio of S_{uu} as a function of the up quark coupling y_{uu} , for $m_\chi = M_S/4$ and $y_\chi/y_{uu} = 2, 1, 1/2$ or 0.

The flavor symmetry introduced in Section II A allows the interactions (2.7) only if χ_R and χ_L have the same transformation property as u_R under the global $U(1)$. For simplicity, we assume that a coupling of S_{uu} to a χ and an up quark has a negligibly small coefficient. This can be a consequence of an approximate Z_2 symmetry, given by invariance under the $\chi \rightarrow -\chi$ transformation. As a result, a $\bar{\chi}_L u_R$ mass mixing is suppressed.

The mass of χ is chosen to satisfy $m_\chi < M_S/2$, so that the interactions Eq. (2.7) lead to a diquark decay into two vectorlike quarks. The LO partial width is given by

$$\Gamma(S_{uu} \rightarrow \chi\chi) = \frac{1}{32\pi} (y_{\chi R}^2 + y_{\chi L}^2) M_S \left(1 - \frac{2m_\chi^2}{M_S^2}\right) \left(1 - \frac{4m_\chi^2}{M_S^2}\right)^{1/2}. \quad (2.8)$$

This partial width and the one given in Eq. (2.3) give the branching fractions of $S_{uu} \rightarrow \chi\chi$ and $S_{uu} \rightarrow uu$ shown in the left panel of Figure 2 for two values of the mass ratio M_S/m_χ . The width-to-mass ratio of S_{uu} is shown in the right panel of Figure 2 for four values of $\sqrt{y_{\chi R}^2 + y_{\chi L}^2}/y_{uu}$.

The diquark interaction with the vectorlike quark in Eq. (2.7) is invariant under the $\chi \rightarrow -\chi$ transformation. If this Z_2 symmetry were not broken by other Lagrangian terms, then the vectorlike quark would be stable. We assume that the dominant Z_2 -breaking interaction is a dimension-5 operator:

$$\frac{C_g}{M_\star} S_{uu} \bar{u}_R \gamma^\mu \gamma^\nu T^a \chi_L G_{\mu\nu}^a + \text{H.c.}, \quad (2.9)$$

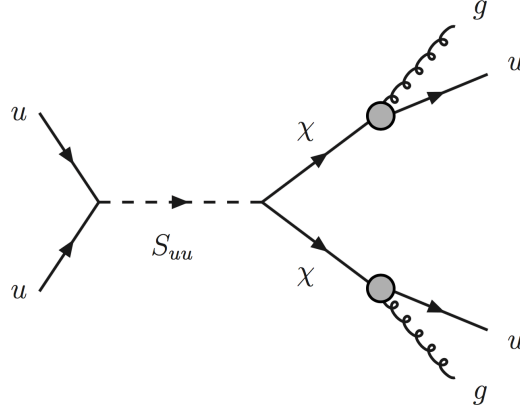


FIG. 3: Diquark production followed by decay into a pair of vectorlike quarks, each of them then decaying at one loop into a gluon and an up quark.

where $G_{\mu\nu}^a$ is the gluon field strength, T^a are the $SU(3)_c$ generators, C_g is a dimensionless coefficient, and M_\star is the mass of a very heavy particle which was integrated out. As this operator arises from a loop process, the C_g coefficient is expected to be of the order of $1/(16\pi^2)$ or smaller. The only 2-body decay induced by the dimension-5 operator is $\chi \rightarrow ug$, which leads to a dijet resonance of mass m_χ . Another mechanism for a decay of a vectorlike quark into a gluon and a SM quark is discussed in [31].

If there is some mass mixing between χ and the u_R quark, then χ may also decay into Wd , Zu or h^0u , where h^0 is the SM Higgs boson. If that mixing is negligible, then various exotic decays of χ may have large branching fractions [32]. We will ignore such processes here, so that χ decays into two jets with a branching fraction of close to 100%. Note though that whatever loops induce operator (2.9), there must be similar loop processes with the gluon replaced by a photon or a Z ; the rates of these processes are model dependent, but typically the gluon process has a rate larger by a factor of $3\alpha_s/\alpha \approx 40$. The total width of χ is very small, below 10^{-5} of its mass; nevertheless, the χ decays are prompt for a large range of parameters.

The $S_{uu} \rightarrow \chi\chi \rightarrow (gu)(gu)$ process (see Figure 3) leads to resonant production of a pair of equal-mass dijet resonances. For $M_S \gg m_\chi$, the signal is a pair of wide jets, each with 2-prong substructure. The rate for this process is given by the cross section of Figure 1 multiplied by the branching fraction of Figure 2. Note that the 4-jet resonant signal and the ultraheavy dijet resonance signal are both large for a range of parameters.

There is an additional new-physics contribution to the final state with a pair of dijet

resonances: QCD production of $\chi\bar{\chi}$ leads to nonresonant production of $(gu)(g\bar{u})$. This nonresonant process has a larger cross section than the diquark induced one when $m_\chi \ll M_S$. However, the former process does not lead to a resonance in the invariant mass distribution of the four jets, and also it does not typically produce wide jets with substructure. Thus, the contribution of the nonresonant 4-jet process to the signal of an ultraheavy diquark is negligible. Nevertheless, the nonresonant $\chi\bar{\chi}$ production is constrained by searches for a pair of dijet resonances, leading to a lower limit on the vectorlike quark mass. The NLO cross section for $pp \rightarrow \chi\bar{\chi}$ [30] at the 13 TeV LHC is approximately 120 fb for $m_\chi = 0.8$ TeV, and 82 fb for $m_\chi = 0.9$ TeV. The CMS search of this type with 36 fb^{-1} of data at $\sqrt{s} = 13$ TeV sets a limit $m_\chi \gtrsim 0.9$ TeV (see left panel of Fig. 11 in [34]), while the ATLAS search [35] with a similar amount of data sets a slightly looser limit.

The S_{uu} signal has a large acceptance, $\mathcal{A}_{4j} \approx 0.8$, in a search for an ultraheavy 4-jet resonance, in which it is required that two dijet resonances have approximately equal mass. For a benchmark in the parameter space where $m_\chi = M_S/4$ and $\sqrt{y_{\chi R}^2 + y_{\chi L}^2} = y_{uu} = 2$, the width-to-mass ratio is 7% and the branching fraction $B(S_{uu} \rightarrow \chi\chi) = 43\%$; the cross section times $\mathcal{A}_{4j}B(S_{uu} \rightarrow \chi\chi)$ is then 3.6×10^{-2} fb at $M_S = 10$ TeV, and 1.5×10^{-3} fb at $M_S = 11$ TeV. To estimate the reach in the 4-jet channel, we next compute the background to this process.

D. QCD 4-jet background

The main background to the $pp \rightarrow S_{uu} \rightarrow \chi\chi \rightarrow (gu)(gu)$ signal is QCD production of four jets. For the very large masses of the 4-jet resonance considered here, the dominant production arises from the quark-quark initial states. Furthermore, the final states with two quarks and two gluons have larger contributions than those with three quarks and one anti-quark. Altogether there are twenty Feynman diagrams (ignoring crossing symmetries) contributing to this process, with some representative ones shown in Figure 4.

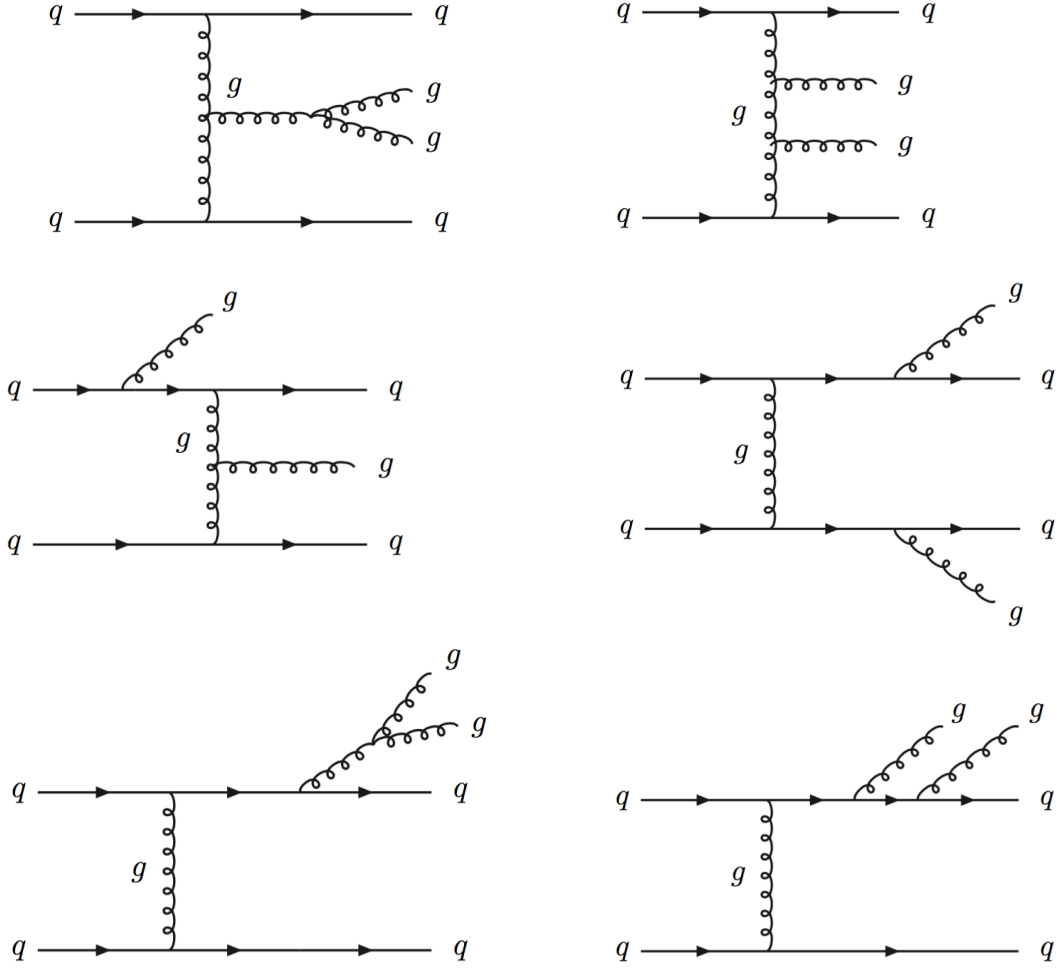


FIG. 4: Representative diagrams for the dominant QCD background to the $4j$ signal, namely quark-quark collisions with two radiated gluons. Eight other diagrams (not taking into account crossing symmetries) similar with the third and fourth diagrams, and six other diagrams similar with the last two are not shown.

We have computed the cross section for the QCD $pp \rightarrow 4j$ process using MadGraph [36] at LO (more precisely MadGraph5_aMC@NLO v2.6) with the following kinematic cuts imposed using MadAnalysis 5 [37]:

- transverse momentum of each jet: $p_{Tj} > 400$ GeV;
- pseudorapidity of each jet: $|\eta_j| < 2.5$;
- separation for each pair of jets: $\Delta R_{jj'} > 0.4$;
- two pairs of jets, with the pair masses satisfying $m_{jj1}, m_{jj2} > 1$ TeV as well as $(m_{jj1} - m_{jj2})/\bar{m}_{jj} < 7\%$, where $\bar{m}_{jj} = (m_{jj1} + m_{jj2})/2$.

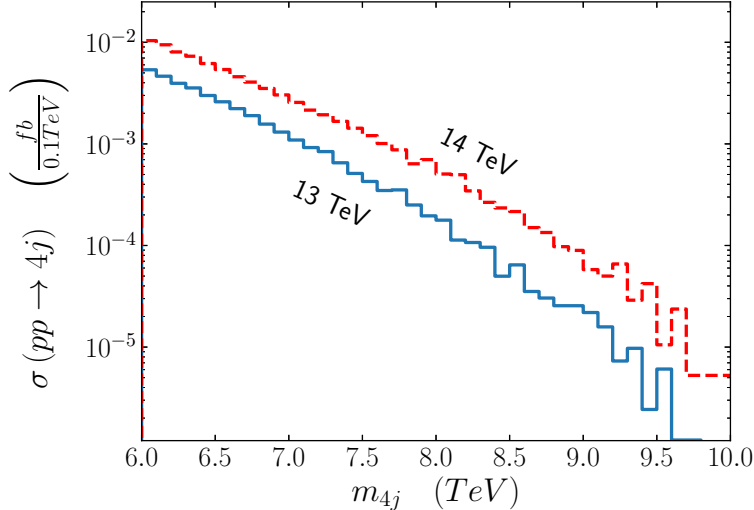


FIG. 5: Cross section for QCD 4-jet production at the LHC at $\sqrt{s} = 13$ TeV and 14 TeV, in mass bins of 100 GeV, as a function of the 4j mass. The cuts imposed on the leading four jets are: $p_{Tj} > 400$ GeV, $|\eta_j| < 2.5$, $\Delta R_{jj'} > 0.4$. In addition, two pairs of jets are each required to have a mass above 1 TeV, and the relative mass difference of the two pairs must be below 7%.

In Figure 5 we show the QCD cross section at LO in mass bins of 100 GeV as a function of the 4-jet invariant mass, obtained with the NNPDF2.3 [28] PDF set at LO. The result with the CT14 set [26] at LO is higher by up to 20%, and the result with the MMHT2014 set [27] at LO is lower by about 15%. To obtain the background in a mass window equal to 8% of the diquark mass, we sum over a number of bins given by $0.8M_S/(1 \text{ TeV})$. This background is smaller by at least three orders of magnitude than the diquark production cross section shown in Figure 1.

An S_{uu} diquark of mass at 11 TeV (see the benchmark in Section II C) may produce four or five 4-jet events with 3000 fb^{-1} of integrated luminosity. Given that the background is below 10^{-2} events, we conclude that a narrow particle as heavy as 11 TeV may be discovered in the 4-jet channel by the end of the high luminosity run of the LHC. This mass reach is lower than that computed in Section II B for the dijet channel due to the smaller value of y_{uu} for fixed width-to-mass ratio, and also the smaller branching fraction.

III. COLORON PLUS SCALAR OR VECTORLIKE QUARK

We now turn to a different theory that includes LHC signals similar to those discussed in the previous section. The ReCoM theory [12, 13] is a gauge extension of QCD to $SU(3)_1 \times SU(3)_2$, with this extended gauge group spontaneously broken by a scalar field Σ which transforms as $(3, \bar{3})$. For a large range of parameters, Σ acquires a VEV that gives the coloron a mass while leaving the gluon massless [38]. All SM quarks transform as triplets under $SU(3)_1$. Below the symmetry breaking scale, the theory consists of the usual QCD with the unbroken gauge group $SU(3)_c$ associated with a massless gluon, plus a massive spin-1 color-octet particle (the coloron) and some scalars particles discussed later on (see Section III B).

The coloron (G') couples to the SM quarks as follows:

$$g_s \tan \theta G'_\mu{}^a \bar{q} \gamma^\mu T^a q \quad , \quad (3.1)$$

where g_s is the QCD gauge coupling (related to the strong coupling constant by $\alpha_s = g_s^2/(4\pi)$), and $\tan \theta$ is the ratio of the $SU(3)_1 \times SU(3)_2$ gauge couplings. The range of $1/5 \lesssim \tan \theta \lesssim 5$ is the one where the theory is perturbative. For $\tan \theta \gtrsim 5$ the coloron coupling to quarks becomes nonperturbative, while for $\tan \theta \lesssim 1/5$ the coloron self-coupling becomes nonperturbative. We focus in this Section on the signals of an ultraheavy coloron.

A. Coloron production

The partial width into SM quark-antiquark pairs, summed over the six SM flavors, is given at LO by

$$\sum_q \Gamma(G' \rightarrow q\bar{q}) = \alpha_s(M_{G'}) \tan^2 \theta M_{G'} \quad . \quad (3.2)$$

We have neglected here the top quark mass, because the corrections are of order $(m_t/M_{G'})^2$, which is below 10^{-3} for a coloron heavier than 6 TeV. The strong coupling constant $\alpha_s(M_{G'})$ at a scale $M_{G'} \approx 6$ TeV is approximately 0.076 if there are no new colored particles lighter than the coloron. Eq. (3.2) implies that the ratio of total width to mass for the coloron satisfies $\Gamma_{G'}/M_{G'} \geq \alpha_s \tan^2 \theta$. As mentioned in Section II A, we are interested in a narrow resonance, that produces a well-defined mass peak. Imposing $\Gamma_{G'}/M_{G'} < 7\%$ sets an upper limit $\tan \theta \lesssim 1$.

The cross section for coloron production is

$$\sigma(pp \rightarrow G') = \frac{2}{s} \int_0^1 \frac{dx}{x} \int_0^{sx} d\hat{s} \sum_q q(x, M_{G'}^2) \bar{q}(\hat{s}/(sx), M_{G'}^2) \hat{\sigma}(q\bar{q} \rightarrow G') , \quad (3.3)$$

where $q(x, Q^2)$ is the PDF of quark $q = d, u, s, c, b$ carrying momentum fraction x , and \hat{s} is the center-of mass energy of the partonic collision. The production cross section at the partonic level is given by [12]:

$$\hat{\sigma}(q\bar{q} \rightarrow G') = \frac{16\pi^2}{9} \alpha_s \tan^2\theta \delta(\hat{s} - M_{G'}^2) . \quad (3.4)$$

The LO production cross section is

$$\sigma(pp \rightarrow G') = \frac{16\pi^2}{9s} \alpha_s \tan^2\theta \int_{M_{G'}^2/s}^1 \frac{dx}{x} \sum_q \left(q(x, M_{G'}^2) \bar{q}(M_{G'}^2/(sx), M_{G'}^2) + q \leftrightarrow \bar{q} \right) . \quad (3.5)$$

The uncertainties in the PDFs are larger in the case of an ultraheavy coloron than those discussed in Section II B. The reason is that the anti-quark PDFs are less constrained at large x . In the case of the NNPDF3.1 [28] set the central value of the predicted cross section is larger than the CT14 [26] one by a factor of about 13 over the mass range $6.5 \text{ TeV} \lesssim M_{G'} \lesssim 9.5 \text{ TeV}$. It appears more reliable to use the CT14 or MMHT2014 [27] PDF sets, which employ a physical parametrization, than the NNPDF3.1 set which is based on neural network fits to the data at significantly smaller x . We also note that the results obtained with the NNPDF sets at NLO or next-to-next-to-leading-order (NNLO) PDF sets are unphysical in some cases: the cross section in Eq. (3.5) is negative for the central values of those sets.

Using Eq. (3.5) and the ManeParse package [39] for reading the PDF files, we find the predicted coloron production cross section at the LHC shown in Figure 6 for the LO CT14 and MMHT2014 PDF sets, including the 1σ -band of the MMHT2014 uncertainties. The NLO corrections to coloron production have been computed in [40, 41]. For $M_{G'}$ above 6 TeV, the LO cross section is enhanced by a factor $K \approx 1.2$. However, the NLO PDF sets at large x lead to a cross section smaller by a factor of 2. Since the NLO PDFs are obtained from fits at much lower energies than those of the ultraheavy regime, we will use only the LO coloron cross section in what follows.

The acceptance for a high-mass vector resonance signal in dijet searches is around 0.4. Using the background estimate discussed at the end of Section II B, we conclude from Figure 6 that for $\tan\theta = 1$ a coloron of mass up to 8 TeV can be discovered as a narrow dijet

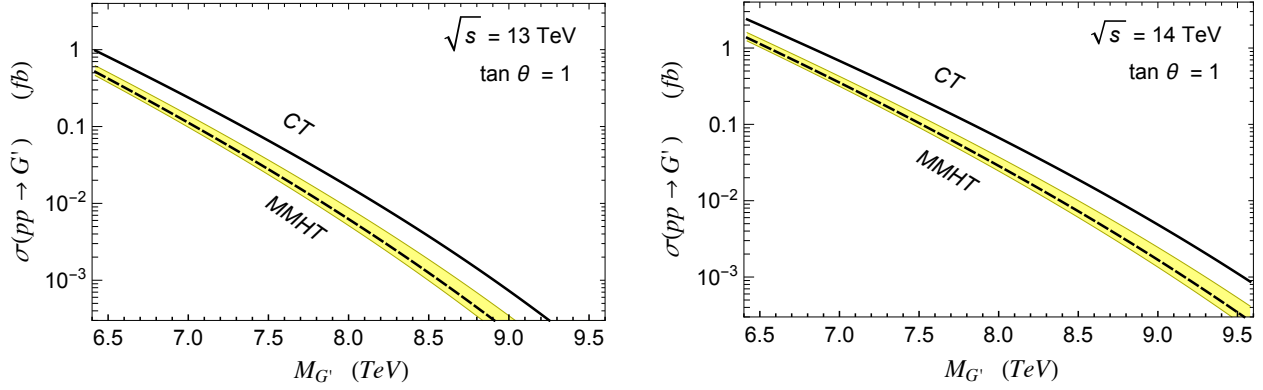


FIG. 6: LO coloron production cross section at $\sqrt{s} = 13$ TeV (left panel) and 14 TeV (right panel), as a function of the coloron mass, for the coloron coupling to quarks equal to that of the gluon ($\tan \theta = 1$). The LO PDF sets used here are CT14 [26] (solid line) and MMHT2014 [27] (dashed line is the central value, shaded band is the uncertainty). The cross section scales as $\tan^2 \theta$.

resonance with 3000 fb^{-1} of data at 14 TeV. If the coloron can decay into new particles, then the mass reach of the LHC may be higher, as we discuss next.

B. Coloron signals with resonant pair of dijets

The scalar field responsible for breaking the extended gauge symmetry, Σ , includes the longitudinal degrees of freedom of the coloron, as well as three physical spin-0 particles [12–15]: a color-octet Θ , a gauge-singlet CP-odd scalar ϕ_I , and a gauge-singlet CP-even scalar ϕ_R . For simplicity, we will assume in what follows that the gauge-singlet scalars are sufficiently heavy so that their production at the LHC can be neglected. We refer to this particular case of the ReCoM as the “coloron+scalar” model.

We also consider an extension of the ReCoM that includes a vectorlike quark, χ , which transforms under $SU(3)_1 \times SU(3)_2$ as $(1, 3)$, while the Θ scalar in this case is assumed heavier than half the coloron mass. We refer to this as the “coloron+quark” model. There is some freedom in choosing the charges of χ under the SM gauge group. For definiteness, we will assume that χ is an $SU(2)_W$ singlet, and has electric charge $+2/3$.

The coupling involving two Θ scalars and one coloron is proportional to the totally-

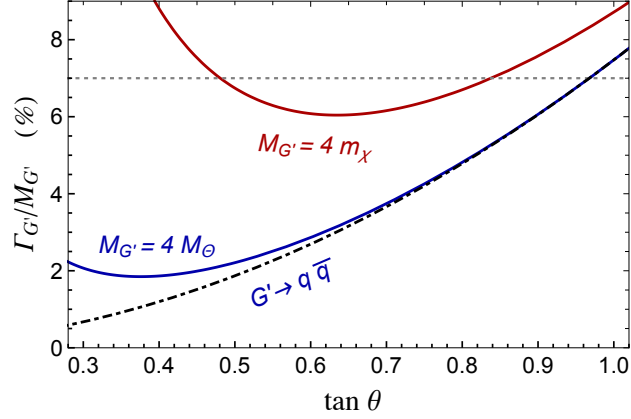


FIG. 7: Ratio of total width to mass for the coloron (G') in the models with color-octet scalar Θ (blue solid line) or vectorlike quark χ (red solid line) of mass $M_{G'}/4$, as a function of the coupling normalization $\tan \theta$. The black dash-dotted line represents the $\Gamma_{G'}/M_{G'}$ ratio when only the decays into SM quarks are kinematically open. The coloron is considered a narrow resonance when its width is below 7% of the mass (marked by the dotted gray line).

antisymmetric color tensor (f^{abc}):

$$-\frac{g_s}{2} (\cot \theta - \tan \theta) f^{abc} G'_\mu{}^a \Theta^b \partial^\mu \Theta^c . \quad (3.6)$$

In the coloron+scalar model, this leads to coloron decays into a pair of Θ scalars with a partial width [13]

$$\Gamma(G' \rightarrow \Theta\Theta) = \frac{1}{32} (\cot^2 \theta - 1)^2 \left(1 - \frac{4M_\Theta^2}{M_{G'}^2}\right)^{3/2} \sum_q \Gamma(G' \rightarrow q\bar{q}) , \quad (3.7)$$

where we used the partial width into quarks given in Eq. (3.2). For $\tan \theta = 1$ this partial width vanishes, as a consequence of the Z_2 symmetry which interchanges the two $SU(3)$ gauge groups. As a result, the total width-to-mass ratio does not surpass 7% for $\tan \theta < 0.95$ (see Figure 7).

In the coloron+quark model, the vectorlike quark χ couples to the coloron proportionally to $1/\tan \theta$:

$$\frac{g_s}{\tan \theta} G'_\mu{}^a \bar{\chi} \gamma^\mu T^a \chi . \quad (3.8)$$

Note that this is different than Eq. (3.1) because χ is a triplet under the second $SU(3)$, while the SM quarks are triplets under the first one. The coloron decay into a pair of vectorlike

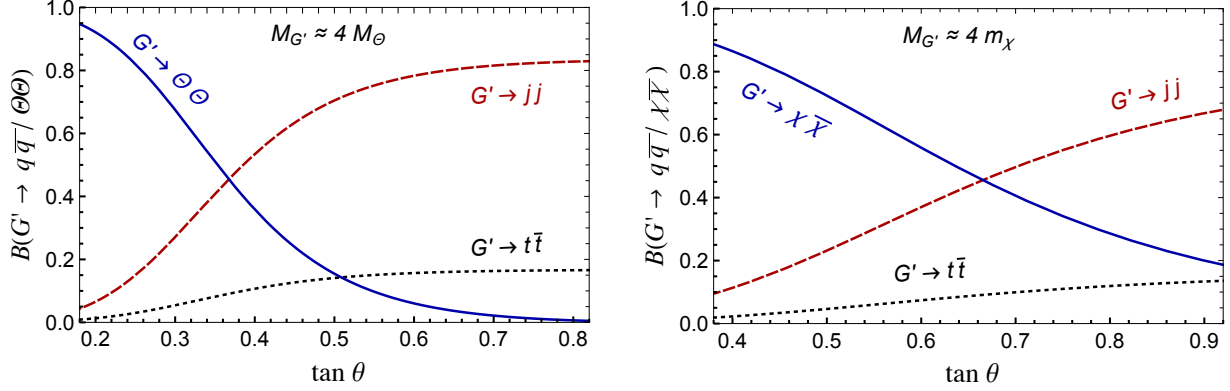


FIG. 8: Branching fractions of the coloron as a function of the coupling normalization $\tan \theta$. The dijet branching fraction (dashed red line) is summed over five $q\bar{q}$ flavors. *Left panel:* Coloron+scalar model with $M_{G'}/M_\Theta \approx 4$. The branching fraction into color-octet scalars (solid blue line) vanishes at $\tan \theta = 1$. *Right panel:* Coloron+quark model with $M_{G'}/m_\chi \approx 4$. The sensitivity to the mass ratio is low, except near threshold ($M_{G'} = 2M_\Theta$ or $M_{G'} = 2m_\chi$).

quarks has a width [42]

$$\Gamma(G' \rightarrow \chi\bar{\chi}) = \frac{1}{6 \tan^4 \theta} \left(1 + \frac{2m_\chi^2}{M_{G'}^2} \right) \left(1 - \frac{4m_\chi^2}{M_{G'}^2} \right)^{1/2} \sum_q \Gamma(G' \rightarrow q\bar{q}) . \quad (3.9)$$

As this is increasing the total width of the coloron, the range of $\tan \theta$ consistent with $\Gamma_{G'}/M_{G'} < 7\%$ becomes $0.5 \lesssim \tan \theta \lesssim 0.8$. The width-to-mass ratio of the coloron is plotted in Figure 7.

These partial widths for $G' \rightarrow \Theta\Theta$ and $G' \rightarrow \chi\bar{\chi}$, together with the $q\bar{q}$ width given in Eq. (3.2) lead to the coloron branching fractions shown in Figure 8. The coloron mass is much larger than the top quark mass, so the branching fraction into quark jets is five times larger than that into a top quark pair. The masses of the color-octet scalar or of the vectorlike quark are closer to $M_{G'}$, so that the phase-space suppression factors in Eqs. (3.7) and (3.9) cannot be neglected. In Figure 8 the mass ratios $M_\Theta/M_{G'}$ and $m_\chi/M_{G'}$ are fixed at 1/4, but for smaller ratios the plots would not change significantly. For larger mass ratios, the decay of the coloron into new particles has smaller branching fractions.

In the coloron+scalar model, the Θ scalar decays into two gluons with a branching fraction of nearly 100%. This decay occurs at one loop, with contributions from both a coloron loop and a Θ loop [13], so the width of Θ is very narrow (nevertheless, the decay is prompt). Thus,

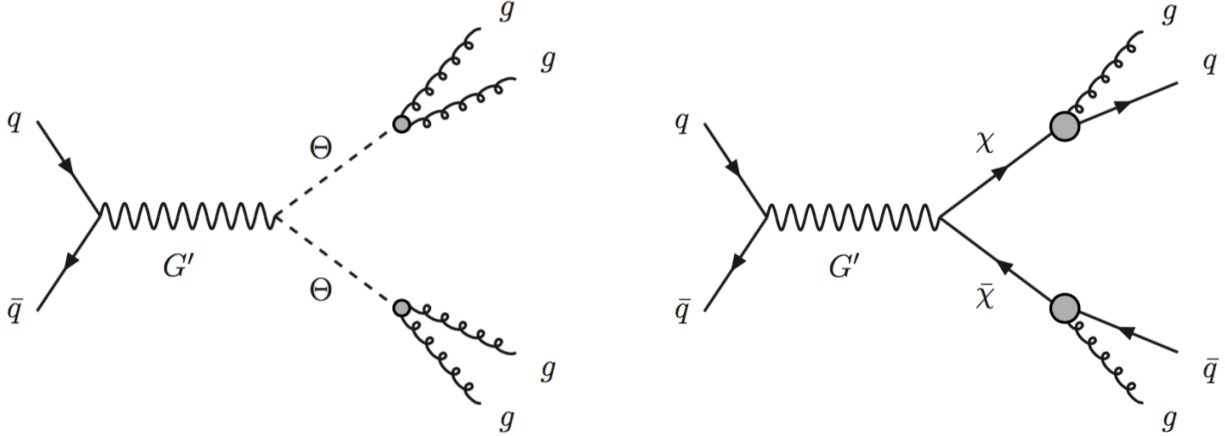


FIG. 9: Coloron production followed by decay into a pair of color-octet scalars (left diagram) or vectorlike quarks (right diagram), each of them then decaying at one loop into two hadronic jets.

the s -channel production of a coloron followed by the cascade decay $G' \rightarrow \Theta\Theta \rightarrow (gg)(gg)$ leads to a pair of dijets (see left diagram of Figure 9). Each dijet has a mass given by M_Θ , and the invariant mass distribution of the four jets has a peak at $M_{G'}$.

For $M_{G'} \gg M_\Theta$ each dijet would appear as a single wide jet with a 2-prong substructure. Consequently, the coloron signal can show up in a dijet resonance search, with the special feature that requiring each wide jet to have substructure can eliminate most of the background.

Given that the Θ scalar carries color, its couplings to gluons lead to nonresonant production of two Θ 's. The process $pp \rightarrow \Theta\Theta \rightarrow (gg)(gg)$ has a larger cross section than $pp \rightarrow G' \rightarrow \Theta\Theta \rightarrow (gg)(gg)$ when $M_\Theta \ll M_{G'}$, but as discussed in Section II C its contribution to the signal of an ultraheavy coloron is negligible. The nonresonant $\Theta\Theta$ production leads though to a lower limit on the scalar mass. The cross section for the nonresonant $pp \rightarrow \Theta\Theta \rightarrow (jj)(jj)$ process at the 13 TeV LHC, including the QCD NLO corrections which induce an increase of about 80% [33], is approximately 130 fb for $M_\Theta = 0.9$ TeV, and 50 fb for $M_\Theta = 1$ TeV. The recent CMS search [34] for a pair of dijet resonances sets a limit $M_\Theta \gtrsim 0.95$ TeV.

In the coloron+quark model, there are various possibilities for the decay of the vectorlike quark χ , as discussed in Section II C. For a simpler comparison with the coloron+scalar model, we assume here that χ decays into two jets with a branching fraction of nearly 100%. This decay may arise from the $\chi \rightarrow ug$ (or cg) process, where the up (or charm) quark and

the gluon are attached to a loop involving some very heavy colored particles. An alternative is the $\chi \rightarrow u\phi_R$ (or $c\phi_R$) process at tree level, with the ϕ_R scalar decaying into two gluons; if ϕ_R is much lighter than χ , then the two gluons are collimated and ϕ_R appears as a single jet. In either case, the $G' \rightarrow \chi\bar{\chi} \rightarrow (jj)(jj)$ process leads to resonant production of a pair of equal-mass dijet resonances. For $M_{G'} \gg m_\chi$, the signal is again a pair of wide jets, each with 2-prong substructure (see right diagram of Figure 9).

The QCD background computed in Section IID (see Figure 5), summed over a number of bins (each of 100 GeV) given by $0.8M_{G'}/1$ TeV is about an order of magnitude smaller than the coloron production cross section shown in Figure 6. Multiplying the latter by $\tan^2\theta$ and by the branching fraction for $G' \rightarrow \Theta\Theta$ or $G' \rightarrow \chi\bar{\chi}$ shown in Figure 8, and by the signal efficiency with the cuts listed in Section IID, we find that the number of signal events is larger than the number of background events as long as $\tan\theta$ is above 0.4 (and not near 1 in the case of the coloron+scalar model). For $\tan\theta \approx 0.6$, a coloron as heavy as 8.5 TeV can be discovered through the $G' \rightarrow \chi\bar{\chi} \rightarrow (jj)(jj)$ process by the end of the high-luminosity run of the LHC.

IV. EVENTS WITH A MASS OF 8 TEV

Experiments at the LHC have recently conducted searches for new particles in both the dijet [6, 18, 25] and 4-jet final states [34, 35]. In this section we explore some hints of an ultraheavy resonance in the data from the dijet resonance searches, and discuss the sensitivity of the 4-jet searches.

A. Dijet and 4-jet LHC searches and events

The CMS experiment has found an event which is a candidate for an ultraheavy resonance decaying into a pair of massive particles. It was reported in the most recent CMS dijet resonance search using 77.8 fb^{-1} of integrated luminosity from 13 TeV pp collisions [6]. The properties of the event, as given in [6], are listed again in Table I. There are four distinct jets in the event reconstructed with the standard jet algorithm used by CMS, the anti- k_T clustering algorithm [43] with a distance parameter $R = 0.4$. The dijet resonance search at CMS uses wide jets (labelled here by J) to reconstruct the dijet mass of the

Dijet Event			Wide Jets			Standard Jets			
Mass (TeV)	$\Delta\eta_{JJ}$	$\Delta\phi_{JJ}$	p_{TJ} (TeV)	Mass (TeV)	ΔR_J	index	p_{Tj} (TeV)	η_j	ϕ_j
8.0	0.4	3.1	3.5	1.8	0.98	0	2.16	0.27	1.47
						2	1.68	0.21	2.45
			3.4	1.8	1.03	1	1.99	0.29	-1.27
						3	1.40	-0.74	-1.17

TABLE I: Properties of the CMS [6] highest-mass dijet event, which contains two wide jets, each made from two standard jets. The quantities of the dijet event are the invariant mass, pseudorapidity separation ($\Delta\eta_{JJ}$), and azimuthal separation ($\Delta\phi_{JJ}$) of the pair of wide jets. The quantities of the wide jets are the transverse momentum (p_{TJ}), the invariant mass (m_J), and the separation (ΔR_J) of the pair of standard jets within each wide jet. The quantities of the standard jets are the p_{Tj} -ordered index, the transverse momentum (p_{Tj}), pseudorapidity (η_j), and azimuthal angle (ϕ_j).

event. The two wide jets are seeded by the corresponding two highest p_T standard jets, and additional jets are included in the two wide jets if they are within a distance $\Delta R_J = \sqrt{(\Delta\eta_J)^2 + (\Delta\phi_J)^2} < 1.1$. The wide jet algorithm is used by CMS to improve the dijet mass resolution in the presence of final state radiation, but it also can reconstruct an ultraheavy resonance decaying to pairs of massive secondary particles. The ultraheavy resonance decay gives a pair of wide jets, where each wide jet is composed of two standard jets resulting from the decay of the secondary particle. The event in Table I has a dijet mass $m_{JJ} \approx 8.0$ TeV, the highest value from CMS so far. In addition to the high dijet mass, the event has a very low probability of being produced by the QCD background, because it has four standard jets, and furthermore each pair of standard jets reconstructs to a large mass of 1.8 TeV. In Section IV B we calculate that the QCD background is below 10^{-4} events.

The CMS experiment has searched for signals of massive dijet resonances and has reported events which are candidates for a new particle of mass near 8 TeV. In addition to the 4-jet event at 8.0 TeV, the CMS search [6] using 77.8 fb^{-1} also reported a typical dijet event with a mass of 7.9 TeV in a dijet mass bin of width 0.3 TeV, giving a total of 2 events observed in

that bin. The estimated QCD background from PYTHIA 8.2 [44] in that bin is 0.6 events. That bin width corresponds to the CMS resolution for a dijet resonance at that mass, so the majority of a signal would generally appear in roughly 2 bins, corresponding to the mass region $7.7 < m_{jj} < 8.3$ TeV. In that region CMS observes 2 events while the background is about 1.1 events, which is a conservative estimate because the background is mainly coming from the lower edge of the mass region not directly underneath the peak. The actual local significance of a dijet resonance signal at 8.0 TeV in that dataset reported by CMS is 1.2 standard deviations. This small but positive significance arises because of the peaking of the signal at 8 TeV, the falling shape of the background, and the inclusion of both the dijet event at 7.9 TeV and the event with the 4-jet topology at 8.0 TeV.

The ATLAS experiment has also searched for massive dijet resonances and has also observed events which are candidates for a new particle of mass near 8 TeV decaying to jj [18]. That search uses only 37 fb^{-1} of integrated luminosity, and the two highest-mass events from ATLAS have a dijet mass of approximately 8.0 and 8.1 TeV. The data from ATLAS is more suggestive of a signal than the data from CMS because those two events are on the tail of the distribution separated from the lower mass events by a gap of about 1 TeV. The ATLAS events are in two adjacent bins, each of width about 0.1 TeV, with a QCD background estimate of only 0.2 events total for those two bins. While 2 events on a background of 0.2 events appears significant, we note that the majority of a resonance signal at ATLAS would appear in more bins than at CMS.¹ Conservatively assuming a similar dijet mass resolution from a resonance for ATLAS as for CMS, we estimate from [18] that the background within the dijet mass interval $7.7 < m_{jj} < 8.3$ TeV for ATLAS is 0.5 events, again coming mainly from the lower edge of the mass interval. So the indications for a dijet resonance at ATLAS at 8 TeV are stronger than at CMS. It would be useful to have an estimate of the local significance of a narrow dijet resonance at 8 TeV from this ATLAS dataset. We note that the ATLAS search for a dijet resonance would not contain a 4-jet event from an 8 TeV resonance, like in Table I, because ATLAS does not use wide jets and instead uses standard jets from the anti- k_T clustering algorithm with a distance parameter $R = 0.5$.

¹ This is because the ATLAS binning corresponds to their calorimeter resolution for the particles inside the dijet, while the CMS binning corresponds to the wider resolution for a dijet resonance, for which the two final state partons can radiate before they hadronize.

The CMS and ATLAS experiments have conducted searches in the 4-jet final state for signals with pairs of dijet resonances. The searches are not very sensitive to a signal from an 8 TeV resonance decaying to secondary particles which in turn decay to dijets. The CMS experiment has conducted a search for pair-produced resonances decaying to quark pairs using 35.9 fb^{-1} of integrated luminosity [34]. The sample of events was recorded during the 2016 run and does not contain the event of Table I which came from the 2017 run. The distribution of the average dijet mass of the two pairs, $\bar{m}_{jj} = (m_{jj1} + m_{jj2})/2$, falls steeply and the highest observed value is $\bar{m}_{jj} \approx 1.6 \text{ TeV}$, smaller than the value $\bar{m}_{jj} = 1.8 \text{ TeV}$ for the event in Table I.

A search for pair-produced dijet resonances from the ATLAS experiment using 36.7 fb^{-1} of integrated luminosity [35] presents a distribution of \bar{m}_{jj} , and a table of signal and background. This search observes 2 events with an expected background of about 2 events for average dijet mass values $\bar{m}_{jj} > 1.79 \text{ TeV}$. Neither the CMS nor the ATLAS searches indicate the observed 4-jet mass, so we cannot tell if any of the events have a 4-jet mass of 8 TeV. The CMS and ATLAS searches integrate over the 4-jet mass and search for signals using only \bar{m}_{jj} , resulting in a much larger background from QCD than would be expected near a 4-jet mass of 8 TeV. Therefore, the reported 4-jet search data from the LHC cannot be used to estimate the QCD background to the event in Table I.

The CMS and ATLAS 4-jet searches were optimized to search for nonresonant pair production of some new colored particle from its QCD couplings, such as a coloron pair [45, 46], or a pair of colored scalars [45, 47]. We propose here a more general search for pair production of dijet resonances at the LHC, exploring the distribution of the 4-jet mass as a function of the average dijet mass of the pairs, which would be sensitive to s-channel production of an ultraheavy resonance.

B. QCD background to resonant production of a pair of dijets

We next estimate the QCD background for the event in Table I. The most restrictive properties of the event are its large 4-jet invariant mass, $m_{4j} = 8 \text{ TeV}$, and the large mass of each of the two wide jets in the event, $m_J = 1.8 \text{ TeV}$. Therefore we calculate the probability of getting an event from QCD with masses equal to or exceeding these values, along with the other cuts imposed by the CMS search.

The QCD 4-jet production at large masses was generically discussed in Section IID. The main contributions arise from quark-quark initial states which radiate two gluons, as shown in Figure 4. We generate the QCD $pp \rightarrow 4j$ process using MadGraph5_aMC@NLO [36], run at LO with $\sqrt{s} = 13$ TeV, using the NNPDF2.3LO [28] parton distributions. The 4-jet cross section has been calculated to NLO in [48], and the K -factor was found to be close to one for large transverse momenta. Therefore, we do not expect the NLO corrections to significantly change the predicted QCD background. Additionally, we expect the effects of the parton shower or hadronization not to exceed 10%, since the observables discussed below are not sensitive to soft or collinear radiation. We will neglect these effects in what follows.

Following the CMS search selection, we apply the CMS wide-jet algorithm to the four final state partons in the event, which are required to be separated by $\Delta R > 0.4$ to mimic the standard anti- k_T algorithm. We also require the two wide jets to be separated in pseudorapidity by $|\Delta\eta_{JJ}| < 1.1$. We produced two samples of 3×10^4 events: one with tight cuts and one with loose cuts. For both samples we additionally place requirements on jet transverse momentum and pseudorapidity which are fully efficient for the QCD background at the large masses discussed here.

The QCD background for the CMS event is computed from the $pp \rightarrow 4j$ sample with tight cuts: $m_{4j} \geq 8$ TeV, $m_{J1} \geq 1.8$ TeV and $m_{J2} \geq 1.8$ TeV. The QCD cross section is 5.7×10^{-7} fb, resulting in 4.5×10^{-5} events expected in 77.8 fb^{-1} of data. Performing PDF reweighting we find that for the CT14 set [26] at LO the cross section is 6.2×10^{-7} fb corresponding to 4.9×10^{-5} events, while for the MMHT2014 set [27] at LO the cross section is 4.8×10^{-7} fb resulting in 3.8×10^{-5} events. We conclude that the Poisson probability of observing the event in Table I from the QCD background alone is approximately 5×10^{-5} , equivalent to a 4 standard deviation excursion of the background.

The QCD cross section has a PDF uncertainty of 21% from NNPDF2.3LO. Note that this uncertainty is relatively small because the dominant contribution only involves valence quarks. The MadGraph simulation also reports that this LO cross section varies by $^{+72\%}_{-40\%}$ when the renormalization (μ_R) and factorization (μ_F) scales are varied by a factor of 2, according to the seven scale scheme, *i.e.*, by finding the maximum excursion in the cross section among the following seven choices of the two scales: $(\mu_F/m_{4j}, \mu_R/m_{4j}) = (0.5, 0.5), (1, 0.5), (0.5, 1), (1, 1), (1, 2), (2, 1), (2, 2)$.

The QCD distributions are studied in the tight sample and also a sample with loose cuts:

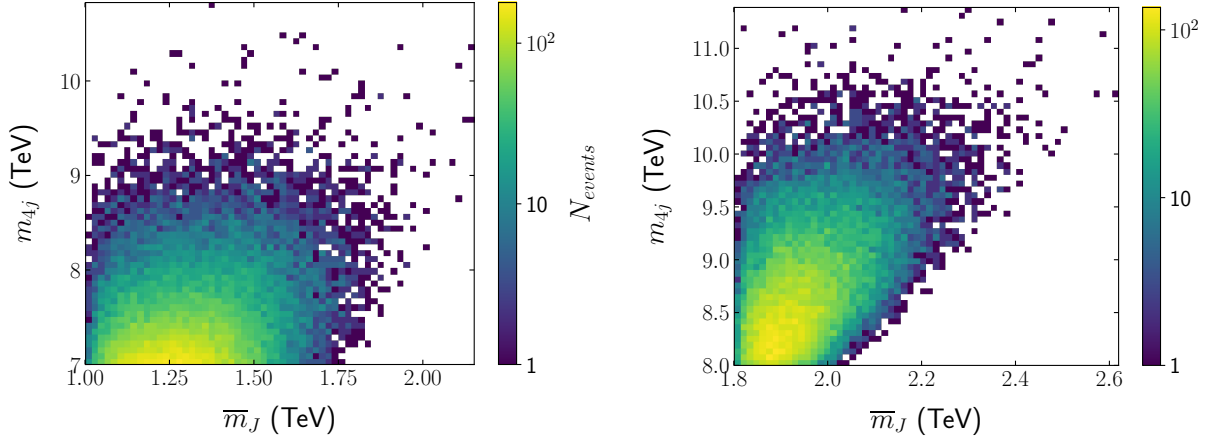


FIG. 10: QCD distribution of the four parton invariant mass (m_{4j}) versus the average diparton mass for the two pairs of partons (\bar{m}_J), from the MadGraph LO samples with the loose cuts (left panel) or tight cuts (right panel) described in the text.

$m_{4j} > 7$ TeV, $m_{J_1} > 1$ TeV and $m_{J_2} > 1$ TeV. In Figure 10 we show the distribution of m_{4j} vs. $\bar{m}_J = (m_{J_1} + m_{J_2})/2$. The distribution falls off rapidly with increasing m_{4j} and \bar{m}_J . We see that background events with high values of both m_{4j} and \bar{m}_J are more rare than events with high values of only one of the two masses, so a search for a massive particle decaying to pairs of dijet resonances using both m_{4j} and \bar{m}_J would be more sensitive than the existing searches at the LHC which have used only one of the two masses.

The diagonal edge to the distributions in Figure 10, *i.e.*, the maximum allowed value of \bar{m}_J which increases with m_{4j} , originates from the kinematics of the $\Delta R_J < 1.1$ requirement for the two partons to be combined into a wide jet. That requirement forces the wide jet mass m_J to be proportional to the wide jet p_T , because $m_J \approx p_{TJ} \Delta R_J/2$ for central jets. However the p_T of the wide jets is limited at a fixed m_{4j} , creating a maximum value of \bar{m}_J for any given value of m_{4j} . In the case where the two wide jets have equal mass, the following approximate relation holds for central jets

$$\bar{m}_J \approx \frac{m_{4j}}{2\sqrt{1 + 4/\Delta R_J^2}} \quad . \quad (4.1)$$

For $m_{4j} = 8$ TeV and a maximum value $\Delta R_{J_{\max}} = 1.1$, we find the maximum allowed value of wide jet mass is $m_{J_{\max}} \approx 1.9$ TeV, from the kinematics estimate alone, which is consistent with the maximum value shown in Figure 10, $m_{J_{\max}} \approx 2$ TeV. Therefore, the wide jet mass of 1.8 TeV for the CMS event in Table I is close to the upper boundary of what is kinematically

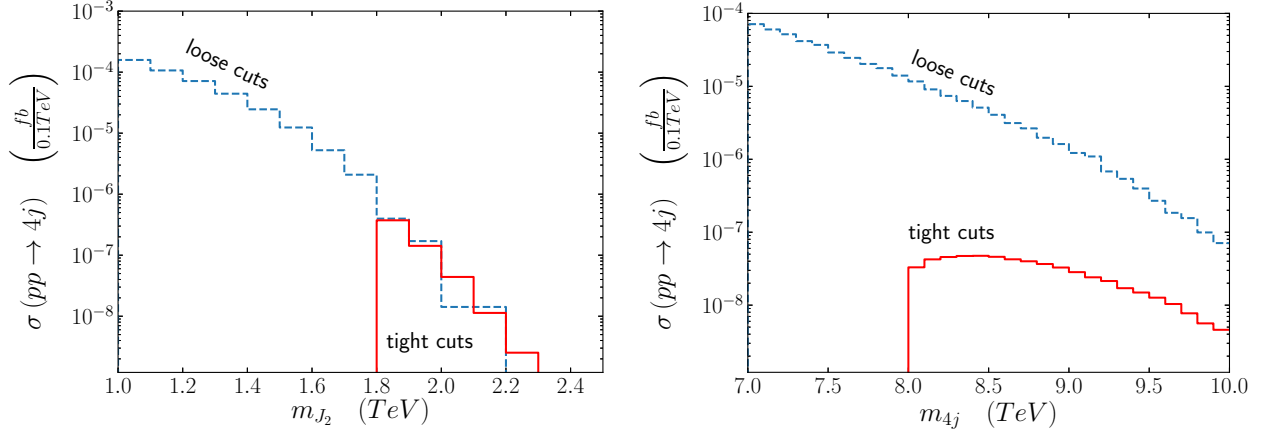


FIG. 11: QCD cross section (in fb/bin) for the $pp \rightarrow 4j$ process at $\sqrt{s} = 13$ TeV computed with MadGraph at LO, as a function of the smaller wide jet mass m_{J_2} in the event (left panel), or of the 4-parton mass m_{4j} (right panel). The results are obtained with the loose cuts (blue dashed line) or tight cuts (red solid line) described in the text.

allowed for the observed 4-jet mass of 8.0 TeV given the wide jet constraint $\Delta R_J < 1.1$. This is similar to the information that the separation of the standard jets in each pair in Table I is $\Delta R_{02} = 0.98$ and $\Delta R_{13} = 1.03$, close to the maximum allowable ($\Delta R_{J_{\max}}$) for the wide jet algorithm.

In Figure 11 we show distributions of the wide jet mass, m_{J_2} , which is the smaller of the two masses, and distributions of m_{4j} . The cross section as a function of m_{J_2} falls significantly faster than m_{4j} . In the tight sample, the m_{J_2} distributions fall off with little bias from the $m_{4j} > 8$ TeV requirement, while the m_{4j} distribution is flattened at low mass by the $m_{J_1}, m_{J_2} > 1.8$ TeV requirements. We see that the latter are more restrictive than the $m_{4j} > 8$ TeV requirement, because QCD events with $m_{J_1}, m_{J_2} > 1.8$ TeV are more rare than those with $m_{4j} > 8$ TeV when the requirement $\Delta R_J < 1.1$ is imposed. In the loose sample, which has the requirements $m_{J_1}, m_{J_2} > 1$ TeV, there is no visible bias in the m_{4j} distribution which falls rapidly as a function of m_{4j} , confirming that the $m_{J_1}, m_{J_2} > 1.8$ TeV cut caused the bias in m_{4j} in the tight sample. This is further supported by the fact that the cross sections for the tight and loose samples for $m_{J_2} > 1.8$ TeV are about the same, again demonstrating that the 4-jet invariant mass cut has a small effect as compared to the wide jet mass cut.

The distributions of the wide jet mass m_{J_1} , which is the larger of the two masses, and of

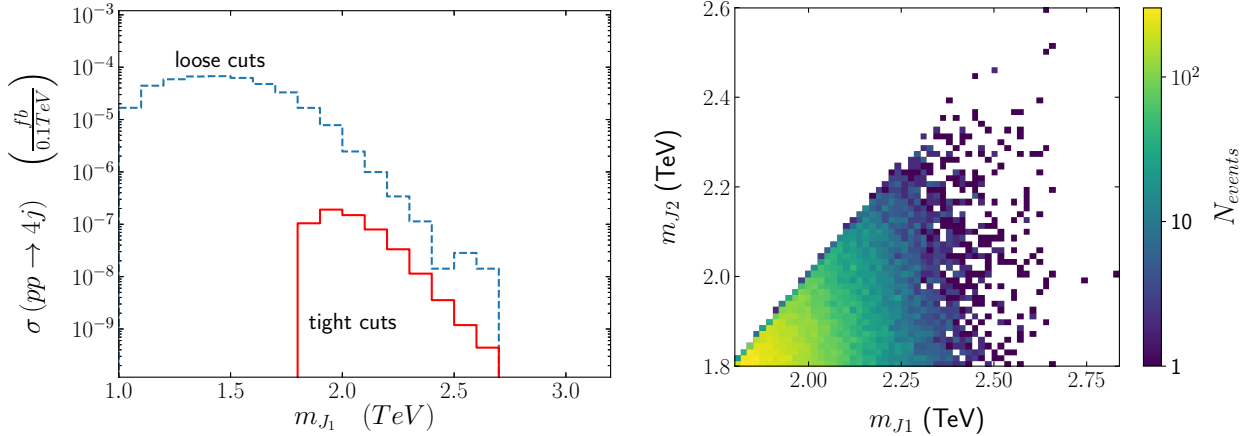


FIG. 12: *Left panel:* same as Figure 11 but for the larger wide-jet mass, m_{J_1} . *Right panel:* the distribution of m_{J_2} vs. m_{J_1} for the sample with tight cuts (see text).

m_{J_2} vs. m_{J_1} are displayed in Figure 12. The wide jet mass m_{J_1} also falls rapidly, like m_{J_2} , but shows a small bias near the $m_{J_1} = 1.8$ TeV cut value caused by requiring $m_{J_1} > m_{J_2}$. We can see that the larger value of wide jet mass m_{J_1} is expected to be within a few hundred GeV of the smaller value of wide jet mass m_{J_2} . We note that the dijet resonance mass resolution at CMS is about 100 GeV for a 1.8 TeV dijet mass. Therefore, the two wide jets are expected to have similar mass values within the expectations from experimental resolution, even when they originate from the QCD background. So the coincidence of observing both wide jets to have a mass of 1.8 TeV in Table I is not as unusual as the large value of that mass. Further, as long as the pairs of jets are constrained to be within the wide jet cone, we do not expect that much enhancement of signal sensitivity could be achieved in an analysis by requiring the two pairs of jets to have the same mass. Loosening the wide jet requirement $\Delta R_J < 1.1$ on the pairs of jets greatly increases the signal efficiency, while the QCD background would still be negligible for the large masses discussed here.

In Figure 13 we show distributions of the wide jet transverse momentum, p_{T_J} , which is the same for both wide jets, and distributions of the pseudorapidity separation of the two wide jets, $\Delta\eta_{JJ}$. Similar to the discussion after Figure 11, the wide jet mass requirements $m_{J_1}, m_{J_2} > 1.8$ TeV in the tight sample, combined with the wide jet clustering requirement $\Delta R_J < 1.1$, constrain the p_{T_J} in the tight sample to be higher than in the loose sample.

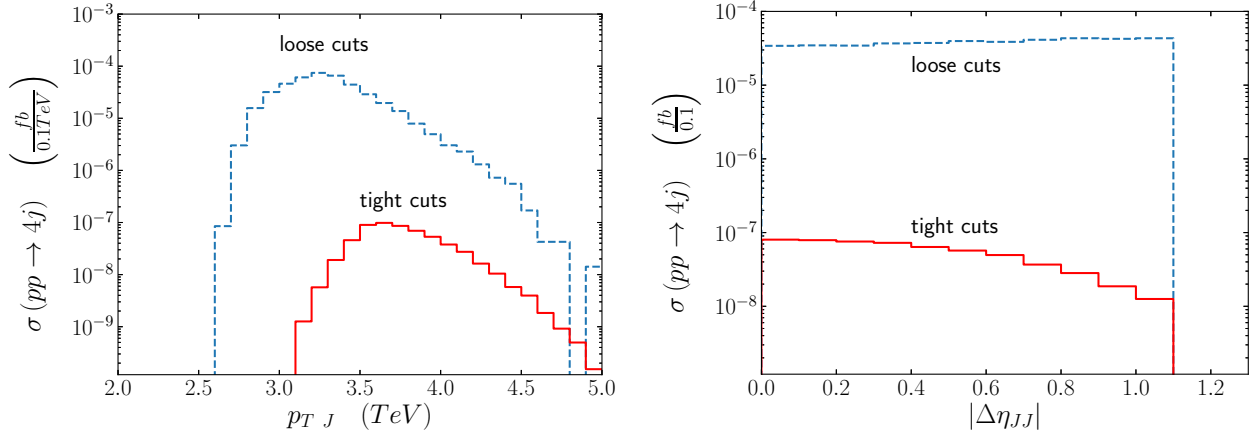


FIG. 13: Same as Figure 11 but for the transverse momentum p_{TJ} of the wide jets (left panel), and for the pseudorapidity separation $|\Delta\eta_{JJ}|$ between the wide jets (right panel).

C. Signals of an 8 TeV particle

Even though there is a single 4-jet event reported so far with an invariant mass of 8 TeV, the tiny probability for QCD to produce that warrants an investigation of what new particles could produce events of this kind. Such an investigation might reveal what additional searches would test the hypothesis that the 8 TeV event is not induced by QCD.

1. S_{uu} diquark with a mass of 8 TeV

The diquark scalar S_{uu} studied in Section II is a prime candidate for producing events at very high mass. We consider the decay of S_{uu} into two vectorlike quarks, which has a large branching fraction. Each vectorlike quark then decays into ug , producing two jets, as discussed in section II C. This leads exactly to the topology of the 8 TeV 4-jet event. We now study the parameter values that are consistent with this $pp \rightarrow S_{uu} \rightarrow \chi\chi \rightarrow 4j$ process as the origin of the 4-jet event.

The masses of the new particles are given by $M_S = 8$ TeV and $m_\chi = 1.8$ TeV. The other important parameters are the couplings y_{uu} , which sets the overall production rate, and $\sqrt{y_{\chi R}^2 + y_{\chi L}^2}$, which determines the branching fraction for $S_{uu} \rightarrow \chi\chi$. As explained in Section II C, we take the branching fraction for $\chi \rightarrow jj$ to be nearly 100%.

For simplicity, we set $y_{\chi L} = 0$ in what follows. Note that the $U(1)$ flavor symmetry

discussed in Section II A can forbid the S_{uu} coupling to χ_L in Eq. (2.7), provided the mass of the vectorlike quark arises from a Yukawa coupling to the $U(1)$ breaking scalar: $\phi_u \bar{\chi}_L \chi_R$. Thus, the only parameters that remain to be fitted to the data are y_{uu} and y_{χ_R} .

For $M_S = 8$ TeV, the NLO cross section at $\sqrt{s} = 13$ TeV is

$$\sigma_8(pp \rightarrow S_{uu}) \approx 0.88 y_{uu}^2 \text{ fb} , \quad (4.2)$$

and the S_{uu} branching fraction relevant for the $4j$ final state when $m_\chi = 1.8$ TeV is

$$B_8(S_{uu} \rightarrow \chi\chi) \approx \left(1 + 1.25 \frac{y_{uu}^2}{y_{\chi_R}^2} \right)^{-1} , \quad (4.3)$$

where the factor of 1.25 is due to the m_χ/M_S dependent factors in the width for $S_{uu} \rightarrow \chi\chi$ given in Eq. (2.8). Note that the model allows in principle a signal rate much larger than that required to explain the $4j$ event observed in the CMS dijet search. For example, $y_{uu} = y_{\chi_R} = 2$ corresponds to $\Gamma_S/M_S \approx 7\%$ and the $\sigma_8(pp \rightarrow S_{uu})B_8(S_{uu} \rightarrow \chi\chi) \approx 1.5$ fb, so the expected number of 8 TeV $4j$ events in 77.8 fb^{-1} could have been substantially larger than 1.

A constraint we need to study is the absence of events involving pairs of dijet resonances with a mass of 1.8 TeV in the dedicated searches of that type. The latest CMS search [34] for pairs of dijets included only the 2016 dataset, so it could not observe the 4-jet event with a pair of dijets at 1.8 TeV recorded in the 2017 dataset (observed in the dijet resonance search [6]). Nevertheless, the absence of events at 1.8 TeV in that search sets an upper bound on the cross section for $pp \rightarrow S_{uu} \rightarrow \chi\chi$. The similar search from ATLAS [35] is less sensitive to our signal because of a kinematic cut which requires the jets within each pair to be highly separated.

Using the MadGraph event generator [36], with model files created by FeynRules [49], we simulated a diquark of mass equal to 8 TeV undergoing decays into a pair of vectorlike quarks that produce dijet resonances of 1.8 TeV, and we determined the parton-level acceptances of the CMS search [34] for pairs of dijets. The results are shown in Table II, where each row includes the combined acceptance for all the requirements above and within that row. We list only those requirements that have less than full acceptance. The requirements that each of the four jets has a transverse momentum $p_{Tj} > 80$ GeV and a pseudorapidity $|\eta_j| < 2.5$ have a high acceptance. The requirement that the mass asymmetry between two pairs of jets is small, $M_{\text{asym}} = (m_{J1} - m_{J2})/(m_{J1} + m_{J2}) < 0.1$, has an acceptance of about 0.9. Finally,

Pair of dijet search requirement	Acceptance (%)		
	$S_{uu} \rightarrow \chi\chi$	$G' \rightarrow \chi\bar{\chi}$	$G' \rightarrow \Theta\Theta$
$p_{Tj} > 80$ GeV	98.4	98.3	98.4
$ \eta_j < 2.5$	94.1	93.0	96.8
$M_{\text{asym}} < 0.1$	80.9	83.6	89.4
$ \Delta\eta_{JJ} < 1$	40.4	36.1	59.1

TABLE II: Cut flow for signals of a diquark (S_{uu}) or a coloron (G') with mass of 8 TeV decaying to pairs of particles with mass of 1.8 TeV, each decaying into two jets. The percentage of events accepted is shown after applying each of the selection requirements from the CMS search [34] for pairs of dijets.

the requirement on the pseudorapidity separation between the dijet pairs, $|\Delta\eta_{JJ}| < 1.0$, has a smaller acceptance which depends on the angular distribution of the model.

We find that the S_{uu} signal acceptance for the kinematic cuts imposed in the CMS search [34] is approximately 0.4, as can be seen in Table II. The nonobservation of 4-jet events with two dijet masses near 1.8 TeV implies, based on Poisson statistics, that the upper limit at the 95% CL on the predicted number of signal events is 3. The amount of data analyzed in that CMS search is 35.9 fb^{-1} . Thus, the upper limit on the cross section times branching fraction is

$$\sigma_8(pp \rightarrow S_{uu}) B_8(S_{uu} \rightarrow \chi\chi) < 0.21 \text{ fb} \quad . \quad (4.4)$$

From Eqs. (4.2) and (4.3) it follows that the above limit translates into a constraint on the following combination of diquark couplings:

$$f(y_{uu}, y_{\chi R}) \equiv y_{uu} \left(1 + 1.25 \frac{y_{uu}^2}{y_{\chi R}^2} \right)^{-1/2} < 0.49 \quad . \quad (4.5)$$

Let us now turn to the CMS dijet resonance search [6] that observed the 8 TeV 4-jet event. The parton-level signal acceptance of the CMS search for reconstructing a resonance of mass equal to 8 TeV decaying to pairs of wide jets is shown in Table III. First, the requirement that each of the four standard jets in the final state satisfies $|\eta_j| < 2.5$ has an acceptance above 0.93. We then apply the CMS wide jet algorithm associating the third and fourth jets to the closest of the two leading jets, and require that this association results

CMS dijet search requirement	Acceptance (%)		
	$S_{uu} \rightarrow \chi\chi$	$G' \rightarrow \chi\bar{\chi}$	$G' \rightarrow \Theta\Theta$
$ \eta_j < 2.5$	94.6	93.5	97.3
Dijet pairs	69.2	69.0	75.3
$ \Delta\eta_{JJ} < 1.1$	44.3	38.9	58.8
$\Delta R_J < 1.1$	8.3	9.4	14.0

TABLE III: Cut flow for signals of ultraheavy resonances decaying to pairs of dijets reconstructed as wide jets. The percentage of events accepted after applying each of the selection requirements for an ultraheavy resonance of mass 8 TeV decaying to pairs of particles of mass 1.8 TeV.

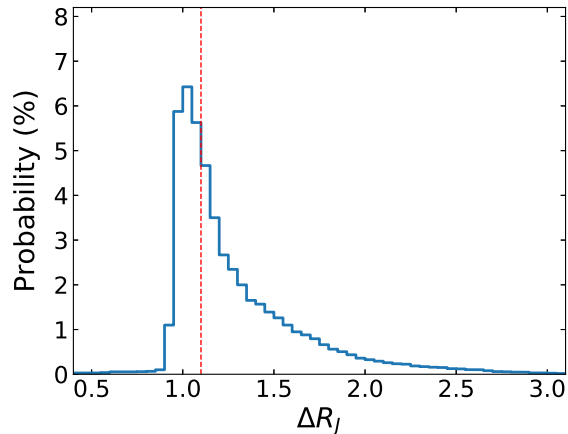


FIG. 14: The separation ΔR_J of the two standard jets within a wide jet produced by the $\chi \rightarrow jj$ decays for events originating from $S_{uu} \rightarrow \chi\chi$, in the model with a diquark of mass $M_S = 8$ TeV and a vectorlike quark of mass $m_\chi = 1.8$ TeV. Only the first three selection cuts from Table III have been imposed. The dotted red line denotes the location of the upper limit of the ΔR_J cut.

in two pairs of dijets, rejecting events where there is a cluster of three jets within a wide jet. The acceptance for this requirement, shown by the row labelled “Dijet pairs” in Table III, is roughly 3/4. Next we require the two clusters of jets have a pseudorapidity separation $|\Delta\eta_{JJ}| < 1.1$, which has an acceptance which again depends on the angular distribution.

Finally, we apply the CMS requirement on the separation between the jets in each wide jet, $\Delta R_J < 1.1$, which has an acceptance of about 0.2. The reason for this low acceptance can be seen from the ΔR_J distribution in Figure 14. The distribution peaks at $\Delta R_J \approx 1.1$

and has a long tail to larger values of ΔR_J , so the wide jet requirement $\Delta R_J < 1.1$ is too tight for this search. The acceptance can be significantly increased by relaxing this cut or replacing the CMS wide jet algorithm with one optimized for a 4-jet signal of an ultraheavy resonance. The final acceptance of the 4-jet analysis (see Table II) is substantially larger than the acceptance of the dijet analysis (see Table III), mainly because the $\Delta R_J < 1.1$ requirement for wide jets is only applied in the dijet analysis.

The diquark signal can produce the CMS 4-jet event with a reasonable probability even considering the constraint from the 4-jet search. Given the acceptance of 8.3% for the S_{uu} signal and the constraint (4.4) from the absence of events in the 4-jet search, we find that the maximum number of expected 4-jet events in the CMS dijet search with 77.8 fb^{-1} of data is $N_{4j}^{\text{exp}} \approx 1.3$. In that case the probability for observing at least one event is 73%. It is perhaps more illuminating to determine what is the maximum probability P_{max} for having at least one 4j event in the dijet search and no events in the pair-of-dijets search. We find $P_{\text{max}} \approx 14\%$, which is obtained for $\sigma_8(pp \rightarrow S_{uu}) B_8(S_{uu} \rightarrow \chi\chi) \approx 5.8 \times 10^{-2} \text{ fb}$, or equivalently for $f(y_{uu}, y_{\chi_R}) \approx 0.26$, where f is the function defined in Eq. (4.5). The above probabilities, 73% and 14%, assume no correlation between the results of the 4-jet search and the dijet search. If there was complete correlation between the observation of zero events in the 4-jet search and in the first 35.9 fb^{-1} of the dijet search, the above probabilities would be reduced to 50% and 8%, respectively.

Let us illustrate the event rates by choosing a benchmark in the parameter space: $y_{uu} = 0.3$, $y_{\chi_R} = 0.5$, corresponding to $f(y_{uu}, y_{\chi_R}) = 0.25$. This implies $B_8(S_{uu} \rightarrow \chi\chi) \approx 69\%$ and $\sigma_8(pp \rightarrow S_{uu}) \approx 8.0 \times 10^{-2} \text{ fb}$. The expected number of 4-jet signal events is then $N_{4j}^{\text{exp}} \approx 0.34$ in the CMS dijet search, and $N_{2 \times 2j}^{\text{exp}} \approx 0.79$ in the CMS pair of dijets search. The expected number of signal jj events in the CMS+ATLAS searches (with a total of $77.8 + 37.0 \text{ fb}^{-1}$) is $N_{jj}^{\text{exp}} \approx 1.4$. Note that the diquark is very narrow, with a total width for this benchmark given by $\Gamma_S \approx 23 \text{ GeV}$, *i.e.*, $\Gamma_S/M_S \approx 0.4\%$.

Similar agreement with the data is obtained for a range of coupling values. For example, $y_{uu} = 0.35$, $y_{\chi_R} = 0.7$, corresponding to $f(y_{uu}, y_{\chi_R}) = 0.31$, gives $B_8(S_{uu} \rightarrow \chi\chi) \approx 76\%$ and $\sigma_8(pp \rightarrow S_{uu}) \approx 0.11 \text{ fb}$, corresponding to $N_{4j}^{\text{exp}} \approx 0.52$, $N_{2 \times 2j}^{\text{exp}} \approx 1.2$ and $N_{jj}^{\text{exp}} \approx 1.5$. We conclude that the model with a scalar diquark and a vectorlike quark can account for all observations, and has a probability of fitting the data which is more than three orders of magnitude higher than in the case of the SM.

To further optimize the search for an 8 TeV resonance decaying to a pair of particles of mass 1.8 TeV at the LHC, we propose a search in the m_{4j} versus \bar{m}_{jj} plane. The pairs of standard jets should be chosen to minimize the pair mass asymmetry, and we find this procedure increases the signal acceptance to 100% at the parton level for the existing CMS cut $M_{asym} < 0.1$. The imposition of the ΔR_{JJ} and $\Delta\eta_{JJ}$ cuts is not required to reduce the negligible QCD backgrounds near the interesting values of m_{4j} and \bar{m}_{jj} . As both cuts significantly reduce the acceptance for signal events, these requirements should either be dropped or substantially relaxed.

2. Other models

The coloron discussed in Section III may also produce events with the topology of the observed ones at 8 TeV. The processes $pp \rightarrow G' \rightarrow \Theta\Theta \rightarrow 4j$ (in the coloron+scalar model) or $pp \rightarrow G' \rightarrow \chi\bar{\chi} \rightarrow 4j$ (in the coloron+quark model) may generate the 4-jet event for $M_{G'} = 8$ TeV and a color-octet scalar of mass $M_\Theta = 1.8$ TeV, or a vectorlike quark of mass $m_\chi = 1.8$ TeV. Dijet events near 8 TeV are also generated by the $pp \rightarrow G' \rightarrow q\bar{q}$ process.

To find the rates for these processes, we multiply the coloron production cross section at the 13 TeV LHC from Figure 6 by the branching fractions from Figure 8. The result is shown in Figure 15, where it is evident that the cross section times branching fraction for the 4-jet final state has a theoretical upper limit: 1.1×10^{-3} fb for $pp \rightarrow G' \rightarrow \Theta\Theta$ at $\tan\theta = 0.34$, and 3.4×10^{-3} fb for $pp \rightarrow G' \rightarrow \chi\bar{\chi}$ at $\tan\theta = 0.64$.

The acceptance for these processes in the CMS dijet analysis is given in Table III: 14% in the case of $G' \rightarrow \Theta\Theta$, and 9.4% in the case of $G' \rightarrow \chi\bar{\chi}$. The maximum cross section times branching fraction, multiplied by the acceptance and the amount of data (77.8 fb^{-1}), then gives the largest expected number of events: $N_{4j}^{\text{exp}} \approx 0.012$ in the coloron+scalar model, and $N_{4j}^{\text{exp}} \approx 0.025$ in the coloron+quark model. Thus, the probability for the 8 TeV 4-jet event to be due to a cascade decay of the coloron is at most 2.5%. Despite being a low probability, this is larger by more than two orders of magnitude than the probability predicted in the SM. If $pp \rightarrow G' \rightarrow \chi\bar{\chi}$ is indeed the origin of the 4-jet event, the probability for observing a second event of this type in 300 fb^{-1} of data at $\sqrt{s} = 13$ TeV is at most 9%. At $\sqrt{s} = 14$ TeV, the coloron production cross section is larger by a factor of 4.0 when the CT14 PDF set is used, and of 4.5 when the MMHT2014 set is used.

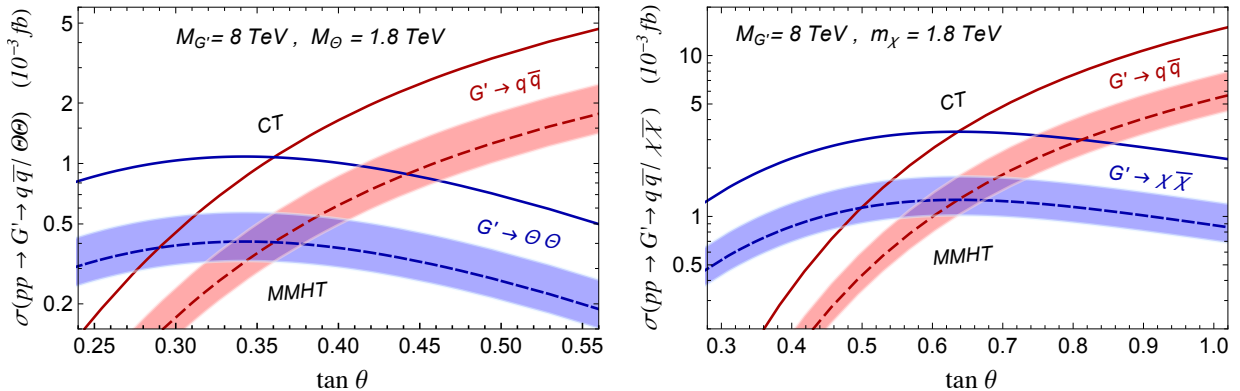


FIG. 15: Cross section times coloron branching fractions at the 13 TeV LHC for $G' \rightarrow \Theta\Theta$ (left panel, blue lines) or $G' \rightarrow \chi\bar{\chi}$ (right panel, blue lines), and for $G' \rightarrow q\bar{q}$ summed over six flavors (red lines), as a function of the coupling normalization $\tan\theta$. The computation is at LO with $M_{G'} = 8$ TeV and $M_{\Theta} = 1.8$ TeV (in the coloron+scalar model, left panel) or $m_{\chi} = 1.8$ TeV (in the coloron+quark model, right panel). Two PDF sets at LO are used here: solid lines correspond to the CT14 set, while the dashed lines and the shaded bands correspond to the central value and uncertainty of the MMHT2014 set, respectively.

There is a larger contribution from the $pp \rightarrow G' \rightarrow q\bar{q}$ process to the jj events in the CMS+ATLAS searches, because the acceptance is higher (~ 0.4), and there is more data ($77.8 + 37.0$ fb $^{-1}$). In practice, though, that contribution is smaller than the background. Even for $\tan\theta = 0.8$, which in the coloron+quark model saturates the $\Gamma_{G'}/M_{G'} < 7\%$ constraint, the expected number of jj events is only $N_{jj}^{\text{exp}} = 0.35$. Note that despite the large acceptances listed in Table II, the limit from the search of a pair of dijets is rather weak due to the small rates in the coloron models.

We have focused here only on a couple of renormalizable coloron models. Nevertheless, it appears challenging to construct selfconsistent and viable coloron models with substantial larger rates while keeping the width-to-mass ratio below $\sim 7\%$. In the end the limited rate is due to the very small PDFs for antiquarks at large x .

The diquark model discussed earlier in this Section is not unique. For example, the vectorlike quarks could decay into an up quark and a boosted spin-0 particle decaying into gg , as mentioned in Section III B. Effectively, this would still lead to a $pp \rightarrow S_{uu} \rightarrow \chi\chi \rightarrow 4j$ process, which could be the origin of the 8 TeV 4-jet event.

The color-sextet diquark scalar S_{uu} has a particularly large production rate because it couples to two up quarks. Diquarks that couple to an up quark and a down quark also have large production cross sections. A color-antitriplet scalar coupled to $u_R d_R$ would generically also couple to $Q_L Q_L$, where Q_L is the SM quark doublet of the first generation. Limits on this type of diquark are explicitly set in the CMS dijet searches [6, 25]. However, its couplings to quark doublets which are connected by the CKM matrix, make this color-antitriplet scalar more likely to induce large flavor-changing processes.

A color-sextet scalar (labelled by S_{ud}) that couples to $u_R d_R$ would not couple to $Q_L Q_L$ due to the antisymmetry of the $SU(2)_W$ indices. An S_{ud} with mass of 8 TeV could generate a 4-jet final state if there are two vectorlike quarks; however, these would have to be approximately degenerate in mass, near 1.8 TeV, which would require fine tuning.

V. CONCLUSIONS

How far can the LHC push the energy frontier? A more specific version of this question is the following: “What are the heaviest particles that could be produced and eventually detected?” In this article we have shown that an S_{uu} diquark, a color-sextet scalar which couples to two up quarks, can be discovered as a narrow dijet resonance, by the end of the high-luminosity run of the LHC, if its mass is as large as 11.5 TeV. For a particle such as a coloron, a color-octet of spin 1 that couples to quark-antiquark pairs, the discovery reach is up to 8.5 TeV.

We have shown that both the diquark and the coloron may decay into a pair of new particles, each of them then decaying into two jets. The ensuing 4-jet signal is substantially larger than the QCD background for ultraheavy resonances (mass above $\sqrt{s}/2$).

We have compared the LHC 4-jet data to models of an ultraheavy resonance. The CMS 4-jet event is a candidate for a diquark with a mass of 8 TeV decaying to a pair of vectorlike quarks with a mass of 1.8 TeV. We have shown that the expected signal at those masses could be as large as 1.3 events in 78 fb^{-1} , corresponding to a probability of 73% of observing at least one event. There is however some tension with the nonobservation of events in a CMS search for nonresonant pairs of dijets. The probability that the diquark produced at least one event in the dijet search and no events in the pair of dijets search can be as large as 14%.

The coloron decay into a pair of vectorlike quarks, or into two color-octet scalars, cannot produce more than about 2.5×10^{-2} events with those masses, making it less likely as an explanation of the CMS event.

The probability for that 4-jet event to be produced by QCD is much smaller, approximately 5×10^{-5} . While the CMS 4-jet event appears unlikely to be due to QCD, a posteriori estimates of the probability of observing one event from the tail of a falling background are inherently biased by the event, so no firm conclusions can be drawn about the significance of a signal unless additional similar events are observed. We have proposed in Section [IV C](#) a search for 4-jet resonances with the jets grouped in pairs of high-mass dijets, which would have a high acceptance for observing the needed additional events to confirm a signal hypothesis.

We have also compared the LHC dijet data to models of an ultraheavy resonance. In addition to the CMS 4-jet event, ATLAS and CMS have reported three other events with only two high p_T jets, which have the reconstructed mass in the range 7.9–8.1 TeV. The QCD background here is more significant, roughly 1.6 events for the sum of both experiments assuming a mass window of 7.7–8.3 TeV. Nevertheless, this leaves room for a signal in the dijet channel, which must be present at some strength if the CMS 4-jet event is also a signal. Assuming the three observed events come from a diquark signal of approximately 1.5 events on the same size QCD background, the branching fractions of the diquark decays would be 70% to a vectorlike quark pair resulting in 4-jet events, and 30% to two up quarks resulting in dijet events. For an optimal search for this class of ultraheavy resonance, dijet searches could be synchronized with the 4-jet searches, and the combined signal significance could be evaluated.

The LHC has the potential to discover an ultraheavy resonance with a cross section beyond the QCD background. The forthcoming runs of the LHC should tell us more about physics at the 10 TeV scale.

Acknowledgments: We thank Niki Saoulidou, Dimitrios Karasavvas, and Melpomeni Diamantopoulou for discussions of the CMS dijet resonance search and the 4-jet event. We also thank Stefan Höche and Stefan Prestel for helpful discussion on the effects of parton showers on the results. This work was supported by Fermi Research Alliance, LLC, under Contract No. DE-AC02-07CH11359 with the U.S. Department of Energy, Office of Science, Office of High Energy Physics.

-
- [1] T. Han, I. Lewis and Z. Liu, “Colored resonant signals at the LHC: Largest rate and simplest topology,” *JHEP* **1012**, 085 (2010) [arXiv:1010.4309 [hep-ph]].
- [2] R. M. Harris and K. Kousouris, “Searches for Dijet Resonances at Hadron Colliders,” *Int. J. Mod. Phys. A* **26**, 5005 (2011) [arXiv:1110.5302 [hep-ex]].
- [3] B. A. Dobrescu and F. Yu, “Coupling-mass mapping of dijet peak searches,” *Phys. Rev. D* **88**, no. 3, 035021 (2013) Erratum: [*Phys. Rev. D* **90**, no. 7, 079901 (2014)] [arXiv:1306.2629].
- [4] T. Aaltonen *et al.* [CDF Collaboration], “Search for new particles decaying into dijets in proton-antiproton collisions at $\sqrt{s} = 1.96$ TeV,” *Phys. Rev. D* **79**, 112002 (2009) [arXiv:0812.4036 [hep-ex]].
- [5] V. Khachatryan *et al.* [CMS Collaboration], “Search for resonances and quantum black holes using dijet mass spectra in proton-proton collisions at $\sqrt{s} = 8$ TeV,” *Phys. Rev. D* **91**, no. 5, 052009 (2015) [arXiv:1501.04198 [hep-ex]].
- [6] CMS Collaboration, “Searches for dijet resonances in pp collisions at $\sqrt{s} = 13$ TeV using the 2016 and 2017 datasets”, CMS-PAS-EXO-17-026 (Sept. 2018), <https://inspirehep.net/record/1693731>
- [7] N. Assad, B. Fornal and B. Grinstein, “Baryon number and lepton universality violation in leptoquark and diquark models,” *Phys. Lett. B* **777**, 324 (2018) [arXiv:1708.06350 [hep-ph]].
- [8] R. N. Mohapatra, N. Okada and H. B. Yu, “Diquark Higgs at LHC,” *Phys. Rev. D* **77**, 011701 (2008) [arXiv:0709.1486 [hep-ph]].
- C. R. Chen, W. Klemm, V. Rentala and K. Wang, “Color Sextet Scalars at the CERN Large Hadron Collider,” *Phys. Rev. D* **79**, 054002 (2009) [arXiv:0811.2105 [hep-ph]].
- J. M. Arnold, M. Pospelov, M. Trott and M. B. Wise, “Scalar Representations and Minimal Flavor Violation,” *JHEP* **1001**, 073 (2010) [arXiv:0911.2225 [hep-ph]].

- [9] T. Han, I. Lewis and T. McElmurry, “QCD corrections to scalar diquark production at hadron colliders,” *JHEP* **1001**, 123 (2010) [arXiv:0909.2666 [hep-ph]].
- [10] E. L. Berger, Q. H. Cao, C. R. Chen, G. Shaughnessy and H. Zhang, “Color sextet scalars in early LHC experiments,” *Phys. Rev. Lett.* **105**, 181802 (2010) [arXiv:1005.2622 [hep-ph]].
P. Richardson and D. Winn, “Simulation of sextet diquark production,” *Eur. Phys. J. C* **72**, 1862 (2012) [arXiv:1108.6154 [hep-ph]].
Z. L. Liu, C. S. Li, Y. Wang, Y. C. Zhan and H. T. Li, “Transverse momentum resummation for color sextet and antitriplet scalar production at the LHC,” *Eur. Phys. J. C* **74**, 2771 (2014) [arXiv:1307.4341 [hep-ph]].
R. S. Chivukula, P. Ittisamai, K. Mohan and E. H. Simmons, “Color discriminant variable and scalar diquarks at the LHC,” *Phys. Rev. D* **92**, no. 7, 075020 (2015) [arXiv:1507.06676].
- [11] R. S. Chivukula, A. G. Cohen and E. H. Simmons, “New strong interactions at the Tevatron?,” *Phys. Lett. B* **380**, 92 (1996) [hep-ph/9603311].
E. H. Simmons, “Coloron phenomenology,” *Phys. Rev. D* **55**, 1678 (1997) [hep-ph/9608269].
- [12] Y. Bai and B. A. Dobrescu, “Heavy octets and Tevatron signals with three or four b jets,” *JHEP* **1107**, 100 (2011) [arXiv:1012.5814 [hep-ph]].
- [13] Y. Bai and B. A. Dobrescu, “Collider tests of the Renormalizable Coloron Model,” *JHEP* **1804**, 114 (2018) [arXiv:1802.03005 [hep-ph]].
- [14] R. S. Chivukula, A. Farzinnia, J. Ren and E. H. Simmons, “Constraints on the scalar sector of the Renormalizable Coloron Model,” *Phys. Rev. D* **88**, no. 7, 075020 (2013) Erratum: [*Phys. Rev. D* **89**, no. 5, 059905 (2014)] [arXiv:1307.1064 [hep-ph]].
- [15] Y. Bai, S. Lu and Q. F. Xiang, “Hexapod coloron at the LHC,” *JHEP* **1808**, 200 (2018) [arXiv:1805.09815 [hep-ph]].
- [16] Y. Bai and J. Shelton, “Composite octet searches with jet substructure,” *JHEP* **1207**, 067 (2012) [arXiv:1107.3563 [hep-ph]].
- [17] C. Kilic, T. Okui and R. Sundrum, “Colored resonances at the Tevatron: Phenomenology and discovery potential in multijets,” *JHEP* **0807**, 038 (2008) [arXiv:0802.2568 [hep-ph]].
- [18] M. Aaboud *et al.* [ATLAS Collaboration] “Search for new phenomena in dijet events using 37 fb⁻¹ of *pp* collision data collected at $\sqrt{s} = 13$ TeV”, *Phys. Rev. D* **96**, 052004 (2017) [arXiv:1703.09127 [hep-ex]].
- [19] R. N. Mohapatra, “Unification and Supersymmetry: The Frontiers of Quark-lepton Physics,”

- New York, USA: Springer (2003) 421 p.
- [20] C. T. Hill, “Topcolor: Top quark condensation in a gauge extension of the standard model,” *Phys. Lett. B* **266**, 419 (1991).
- [21] B. A. Dobrescu and C. T. Hill, “Electroweak symmetry breaking via top condensation seesaw,” *Phys. Rev. Lett.* **81**, 2634 (1998) [hep-ph/9712319].
R. S. Chivukula, B. A. Dobrescu, H. Georgi and C. T. Hill, “Top Quark Seesaw Theory of electroweak symmetry breaking,” *Phys. Rev. D* **59**, 075003 (1999) [hep-ph/9809470].
H. Collins, A. K. Grant and H. Georgi, “The phenomenology of a top quark seesaw model,” *Phys. Rev. D* **61**, 055002 (2000) [hep-ph/9908330].
H. J. He, C. T. Hill and T. M. P. Tait, “Top quark seesaw, vacuum structure and electroweak precision constraints,” *Phys. Rev. D* **65**, 055006 (2002) [hep-ph/0108041].
- [22] C. Luhn, S. Nasri and P. Ramond, “Simple finite non-Abelian flavor groups,” *J. Math. Phys.* **48**, 123519 (2007) [arXiv:0709.1447 [hep-th]].
- [23] E. C. F. S. Fortes, K. S. Babu and R. N. Mohapatra, “Flavor physics constraints on TeV scale color sextet scalars,” arXiv:1311.4101 [hep-ph].
- [24] R. S. Chivukula, P. Ittisamai, K. Mohan and E. H. Simmons, “Broadening the reach of simplified limits on resonances at the LHC,” *Phys. Rev. D* **96**, no. 5, 055043 (2017) [arXiv:1707.01080].
- [25] A. M. Sirunyan *et al.*, [CMS Collaboration], “Search for narrow and broad dijet resonances in proton-proton collisions at $\sqrt{s} = 13$ TeV and constraints on dark matter mediators and other new particles”, *JHEP* **1808**, 130 (2018) [arXiv:1806.00843 [hep-ex]].
- [26] S. Dulat *et al.*, “New parton distribution functions from a global analysis of quantum chromodynamics,” *Phys. Rev. D* **93**, no. 3, 033006 (2016) [arXiv:1506.07443 [hep-ph]].
- [27] L. A. Harland-Lang, A. D. Martin, P. Motylinski and R. S. Thorne, “Parton distributions in the LHC era: MMHT 2014 PDFs,” *Eur. Phys. J. C* **75**, no. 5, 204 (2015) [arXiv:1412.3989].
- [28] R. D. Ball *et al.* [NNPDF Collaboration], “Parton distributions from high-precision collider data,” *Eur. Phys. J. C* **77**, no. 10, 663 (2017) [arXiv:1706.00428 [hep-ph]].
R. D. Ball *et al.*, “Parton distributions with LHC data,” *Nucl. Phys. B* **867**, 244 (2013) [arXiv:1207.1303 [hep-ph]].
- [29] A. Buckley, J. Ferrando, S. Lloyd, K. Nordström, B. Page, M. Rüfenacht, M. Schönherr and G. Watt, “LHAPDF6: parton density access in the LHC precision era,” *Eur. Phys. J. C* **75**, 132 (2015) [arXiv:1412.7420 [hep-ph]].

- [30] F. Yu, “Di-jet resonances at future hadron colliders: A Snowmass whitepaper,” arXiv:1308.1077 [hep-ph].
- [31] J. H. Kim and I. M. Lewis, “Loop induced single top partner production and decay at the LHC,” JHEP **1805**, 095 (2018) [arXiv:1803.06351 [hep-ph]].
- [32] B. A. Dobrescu and F. Yu, “Exotic signals of vectorlike quarks,” J. Phys. G **45**, no. 8, 08LT01 (2018) [arXiv:1612.01909 [hep-ph]].
- [33] D. Goncalves-Netto, D. Lopez-Val, K. Mawatari, T. Plehn and I. Wigmore, “Sgluon Pair Production to Next-to-Leading Order,” Phys. Rev. D **85**, 114024 (2012) [arXiv:1203.6358].
- [34] A. M. Sirunyan *et al.* [CMS Collaboration], “Search for pair-produced resonances decaying to quark pairs in proton-proton collisions at $\sqrt{s} = 13$ TeV”, CMS-EXO-17-021, arXiv:1808.03124.
- [35] M. Aaboud *et al.* [ATLAS Collaboration], “A search for pair-produced resonances in four-jet final states at $\sqrt{s} = 13$ TeV”, Eur. Phys. J. C **78**, 250 (2018) [arXiv:1710.07171 [hep-ex]].
- [36] J. Alwall, R. Frederix, S. Frixione, V. Hirschi, F. Maltoni, O. Mattelaer, H.-S. Shao, T. Stelzer, P. Torrielli, M. Zaro, “The automated computation of tree-level and next-to-leading order differential cross sections, and their matching to parton shower simulations,” JHEP **1407**, 079 (2014) [arXiv:1405.0301 [hep-ph]].
- [37] E. Conte, B. Fuks and G. Serret, “MadAnalysis 5, a user-friendly framework for collider phenomenology,” Comput. Phys. Commun. **184**, 222 (2013) [arXiv:1206.1599 [hep-ph]].
- E. Conte, B. Dumont, B. Fuks and C. Wymant, “Designing and recasting LHC analyses with MadAnalysis 5,” Eur. Phys. J. C **74**, no. 10, 3103 (2014) [arXiv:1405.3982 [hep-ph]].
- B. Dumont *et al.*, “Toward a public analysis database for LHC new physics searches using MadAnalysis 5,” Eur. Phys. J. C **75**, no. 2, 56 (2015) [arXiv:1407.3278 [hep-ph]].
- [38] Y. Bai and B. A. Dobrescu, “Minimal $SU(3) \times SU(3)$ Symmetry Breaking Patterns,” Phys. Rev. D **97**, no. 5, 055024 (2018) [arXiv:1710.01456 [hep-ph]].
- [39] D. B. Clark, E. Godat and F. I. Olness, “ManeParse: A Mathematica reader for Parton Distribution Functions,” Comput. Phys. Commun. **216**, 126 (2017) [arXiv:1605.08012].
- [40] R. S. Chivukula, A. Farzinnia, E. H. Simmons and R. Foadi, “Production of massive color-octet vector bosons at next-to-leading order,” Phys. Rev. D **85**, 054005 (2012) [arXiv:1111.7261].
- [41] R. S. Chivukula, A. Farzinnia, J. Ren and E. H. Simmons, “Hadron collider production of massive color-octet vector bosons at next-to-leading order,” Phys. Rev. D **87**, no. 9, 094011 (2013) [arXiv:1303.1120 [hep-ph]].

- [42] B. A. Dobrescu, K. Kong and R. Mahbubani, “Prospects for top-prime quark discovery at the Tevatron,” JHEP **0906**, 001 (2009) [arXiv:0902.0792 [hep-ph]].
- [43] M. Cacciari, G. P. Salam, and G. Soyez, “The anti- k_T jet clustering algorithm”, JHEP **0804**, 63 (2008). [arXiv:0802.1189 [hep-ex]].
- [44] T. Sjöstrand *et al.*, “An Introduction to PYTHIA 8.2,” Comput. Phys. Commun. **191**, 159 (2015) [arXiv:1410.3012 [hep-ph]].
- [45] B. A. Dobrescu, K. Kong and R. Mahbubani, “Massive color-octet bosons and pairs of resonances at hadron colliders,” Phys. Lett. B **670**, 119 (2008) [arXiv:0709.2378 [hep-ph]].
- [46] M. Buschmann and F. Yu, “Collider constraints and new tests of color octet vectors,” JHEP **1709**, 101 (2017) [arXiv:1706.07057 [hep-ph]].
- [47] R. S. Chivukula, M. Golden and E. H. Simmons, “Multi - jet physics at hadron colliders,” Nucl. Phys. B **363**, 83 (1991).
- [48] Z. Bern *et al.*, “Four-Jet Production at the Large Hadron Collider at Next-to-Leading Order in QCD,” Phys. Rev. Lett. **109**, 042001 (2012) [arXiv:1112.3940 [hep-ph]].
- [49] A. Alloul, N. D. Christensen, C. Degrande, C. Duhr and B. Fuks, “FeynRules 2.0 - A complete toolbox for tree-level phenomenology,” Comput. Phys. Commun. **185**, 2250 (2014) [arXiv:1310.1921 [hep-ph]].